A Rare Supercell Outbreak in Western Nevada: 21 July 2008

CHRIS SMALLCOMB
National Weather Service, Weather Forecast Office, Reno, Nevada

(Manuscript received 30 June 2009, in final form 29 September 2009)

ABSTRACT

A rare outbreak of organized severe thunderstorms took place in western Nevada on 21 July 2008. This paper will examine the environment antecedent to this event, including unusual values of shear, moisture, and instability. An analysis of key radar features will follow focusing primarily on WSR-88D base data analysis. The article demonstrates several locally developed parameters and radar procedures for identifying severe convection, along with addressing challenges encountered in warning operations on this day.

1. Introduction – Event Synopsis

A rare outbreak of organized severe thunderstorms took place in the National Weather Service (NWS) Reno forecast area (FA) on 21 July 2008. Based on forecaster experience, this has been subjectively classified as a "one in ten" year event for the western Great Basin (WGB), which being located in the immediate lee of the Sierra Nevada Mountains, is unaccustomed to widespread severe weather. Unorganized pulse type convection is a much more frequent occurrence in this portion of the country.

On 21 July 2008, numerous instances of large hail and heavy rainfall were associated with severe thunderstorms (Fig. 1). The maximum hail size reported was half-dollar (3.2 cm, 1.25"), however there is indirect evidence even larger hail occurred. Several credible reports of funnel clouds were received from spotters, though a damage survey the following day found no evidence of tornado touchdowns. During the survey, damage to trees suggested several of these storms produced straight-line winds of approximately 70 mph (31 m sec^{-1}). There were a total of 20 Severe Thunderstorm Warnings, 6 Tornado Warnings, and 2 Flash Flood Warnings issued on

Corresponding author address: Christopher Smallcomb, National Weather Service, 2350 Raggio Parkway, Reno, NV 89512
E-mail: chris.smallcomb@noaa.gov

July 21st in the Reno FA. This is close to half the average annual severe thunderstorm warnings in the Reno FA, occurring on a single day.

An examination of the pre-storm environment will take place in section 2, with an analysis of radar signatures from selected storms in section 3. Brief comments on supplemental soundings and warning challenges on this day will be presented in section 4. Date/time references will use DD/HHMM format; all times are assumed to be UTC. Figure 2 shows key geographical locations referenced in the text.

2. Pre-Storm Environment – Convective Initiation (CI)

As seen in the radar animation of the event (Fig. 1), CI occurred in far western Nevada between roughly 21/1900 and 21/2100, with storms lasting well past 22/0200. Attributable to an exceptionally favorable environment, CI was earlier than is typical in western Nevada.

a. Dynamics-Shear

One of the more prominent aspects to this event was the presence of a compact upper low off the California-Oregon coast (Fig. 3), substantially increasing the vertical wind shear over western Nevada. The 250 hPa wind anomalies (Grumm and Hart 2001) clearly highlight the presence of enhanced winds aloft from northeast California into western Nevada at 22/0000 (Fig. 4), which increased the vertical shear and potential for severe convection.

An analysis of the upper tropospheric forcing identifies the main upper trough as a depression in the dynamic tropopause off the northwest California coastline at 22/0000, with an associated 36-41 m sec^{-1} (70-80 knot) 250 hPa jet streak immediately to the east (Fig. 5). Wallmann (2004) used this technique to forecast dry thunderstorm outbreaks in Nevada by analyzing perturbations along the dynamic tropopause along with upper tropospheric lapse rates. Lift is seen to the north and east of this upper trough center within the dynamic tropopause

pressure advection fields. However it is not until after 22/0000 that the zone of ascent moves into western Nevada, making its direct contribution to CI questionable. Convection formed in typically favored orographic areas of western Nevada and eastern California (e.g. Fig. 2).

An east to west oriented boundary is apparent in a fast loop of visible satellite imagery (Fig. 6). While storms originated along the higher terrain, this boundary was likely a focus for sustaining storms as cells moved away from terrain northeast across western Nevada. The boundary's relatively slow speed compared to faster winds aloft implies it was a lower tropospheric feature. However, the origin and nature of this boundary is uncertain, as the surface to 500 hPa temperature, moisture, and wind fields in LAPS and NAM (not shown) do not exhibit a substantive organization or gradients in that vicinity. LAPS, Local Analysis and Prediction System, is a realtime 3-D analysis system used by all NWS offices. The sparse nature of observations in the area of CI hinders a complete analysis. It is also entirely possible storms formed at the same time on different mountain ranges, and then translated within the mean flow at roughly the same speed, giving the appearance of a boundary.

Forecasters in the WGB have found traditional severe convective parameters and indices which stop at 6 km AGL or 500 hPa do not work well at discriminating severe vs. non severe storms since convection in the region is often based at or above 500 hPa. It is clear in this case that while the 0-6 km shear does not increase between 21/1200 and 21/1800 (Fig. 7), the wind speeds near the equilibrium level (around 8 km AGL) do increase considerably, going from 55 to 70 knots (28 to 36 m sec^{-1}), as the jet streak nears western Nevada. 3-8 km AGL bulk shear increased from 27 to 44 knots (14 to 22 m sec^{-1}) between 21/1200 and 21/1800, leading to greater chances for high based supercell thunderstorms. It should be noted here the 21/1800 special sounding yields an excellent sample of the pre-convective environment, taking place only

1-3 hours before CI. 0-3 km AGL storm relative helicity (SRH) increased from 67 to 126 m^2s^{-2} between the 21/1200 and 21/1800 soundings, primarily due to an increase in the flow speeds at 3 km AGL. This increased the likelihood of mesocyclone development, assuming this low level air could be entrained into the thunderstorms.

b. Moisture

Southerly flow along the periphery of a persistent upper level ridge centered over the Four Corners region led to an increase in moisture over the WGB 2-3 days prior to the event. By the morning of 21 July surface dewpoints of 55-60º F (13-16 C) were noted over much of western Nevada (Fig. 8), which is truly exceptional. Dewpoints began to drop off after 21/1300 with mixing in the daytime boundary layer, yet since a nearly saturated layer existed between 700-500 hPa (Fig. 7) surface dewpoints dropped only into the 45-50º F (7-10 C) range during the afternoon, enhancing instability and resultant convective potential. A true judge of how unusually moist the airmass was can be seen in the precipitable water (PW) anomaly field from the GFS Ensemble Forecast System (GEFS, Fig. 9). PW anomalies greater than +2 SD were noted at 21/1200 as far west as Reno, NV. In a normal Gaussian distribution, anomalies of +2 SD or higher would take place only 2.27% of the time. These anomalously high PW values did increase concern for flash flooding in the WGB based on historical patterns (Brong 2005).

c. Instability

As would be expected, the atmosphere destabilized between 21/1200 and 21/1800 as observed in the Reno soundings both due to a combination of increased surface heating, plus the slight erosion of a small capping inversion seen in the 21/1200 sounding near 500 hPa (Fig. 7). During the daylight hours of 21 July a stability gradient developed across the region, as seen in Figure 10 from the GOES sounder. Comparatively flat cumulus and wave clouds noted in the

visible imagery confirm the more stable atmosphere over the northern Sierra Nevada Mountains (Fig. 6). This contrasts with western Nevada where cloud cover exhibited more vertical development and texture, suggestive of an unstable environment.

A more rapid destabilization occurred in proximity to the Sweetwater Range, where in the LAPS 400 hPa Lifted Indices ($LI_{400\ hPa}$) dropped from near 0 C at 21/1400 to -7.5 C at 21/2000 (Fig. 11). The $LI_{400\ hPa}$ is used in the WGB since it tends to capture capping immediately above 500 hPa, common in this area, which the traditional LI will fail to see (thereby overestimating instability). The 400 hPa Modified Total Totals, an extension of a technique introduced by Milne (2004), uses data at the 700-400 hPa levels with values above 51 C suggestive of enhanced convective potential. These analyses at approximately the time of CI show two key features from the area of CI northeast into central Nevada: 1) significant destabilization with widespread $LI_{400\ hPa}$ values less than -5 C coupled with high Modified Total Totals, and 2) a narrow axis of high downdraft CAPE (DCAPE). Given there we no confirmed tornado touchdowns but several credible spotter reports of funnel clouds were received, it is surmised that cloud base heights and sub-cloud dryness were too excessive for successful tornadogenesis to occur (Markowski et al. 2002).

d. Composite Procedure

A prototype severe convection procedure, as shown in Figures 12a and 12b, has been developed using a blend of nationally and locally developed tools to evaluate the threat of severe thunderstorms and flash flooding in the Reno FA. The procedure made it clear strong shear would be collocated with plentiful moisture and instability over the WGB. Two parameters contained in the procedure not mentioned earlier are now briefly discussed.

Corfidi Vectors (Corfidi et al. 1996), which in the WGB are calculated in the 700 to 300 hPa layer (due to terrain limitations), suggested relatively little potential for flash flooding from back-building convection. As seen in Figure 12a., "modified" Corfidi Vector magnitudes were on the order of 15 to 25 kts (8 to 13 m sec^{-1}), far above the 10 kts (5 m sec^{-1}) or less used as a rough threshold for training/back-building potential in the BUFKIT heavy precipitation diagram. Though storms tended not to back-build on 21 July, the anomalously high PW values still led to locally heavy rainfall with minor flooding.

Even though this was not an MCS event, the MCS Maintenance Probability parameter (Coniglio and Corfidi 2006) appeared to be useful in highlighting the potential for severe convection in this event. Widespread values above 80% were noted in the LAPS data (Fig. 11) near the CI region starting at 21/2000. One reason this parameter may be of particular use in the WGB is that most of the ingredients are in-line with depths of high-based convection in the west. Due to limited experience with the MCS parameter, it is unknown if high values correspond to only severe convective events in the WGB (versus non-severe convection).

3. Radar Analysis – Convective Evolution

a. The "H2" Storm

The "H2" cell, referring to its WSR-88D cell ID (#1 in Fig. 1) formed near the Sweetwater Mountains and was the strongest and longest lasting (~3 hours) of the afternoon. An apparent mesocyclone developed in the 0.5 to 1.9 degree storm-relative velocity scans by 21/2155 (Fig. 13a). It is asserted a non-trivial portion of these circulation signatures were in fact due to inbound velocity data contamination from a three body scatter spike (TBSS), particularly around 21/2208 (Fig. 13b), where the velocity patterns follow similarly those shown in Smallcomb (2006, 2008). The fact the strong inbound velocities follow the general shape of the

TBSS reflectivity signature, are located on the periphery of the storm along the reflectivity gradient, and spectrum width values were moderate to high (not shown) suggests they are related and likely false. These data could easily partially or entirely mask a real mesocyclone within these right-moving thunderstorms, thereby decreasing forecaster confidence in what is being interpreted from the radar data.

A three-dimensional rendition of the 50 dBz isosurface centered at 21/2226 shows a rightward jump due to continuous propagation (Fig. 14). At 21/2243, the cell crossed US Highway 50, approximately 16 miles east of Fallon, NV. The Maximum Estimated Hail Size (MEHS) algorithm from GRLevel 2 (Gibson Ridge Software 2009) indicated a hail size of 1.78 inches (4.5 cm). Based on a storm survey the next day, the maximum hail size at this time was likely closer to 1.00" (2.5 cm) or quarter size. This assessment was based on "hail fossils" found in the mud along Highway 50 (Fig. 15). These fossils, partially solidified in the drying mud, are similar to the markings observed in hailpads (Lozowski and Strong 1978) currently used by several organizations (e.g. CoCoRaHS 2009) for hail stone measurement. This was the only tangible evidence of severe weather from this storm, having passed through some of the most remote sections of Nevada.

Immediately after passing US 50, the cell intensified rapidly as it began interacting with the south end of the Stillwater Range. At 21/2256, a 29 km long TBSS signature was observed in the low-level reflectivity field, associated with a strong inbound velocity anomaly at 21/2301 near the periphery of the highest reflectivity (Fig. 16). Figure 17 shows a large area of 50+ dBz reflectivity in the LRM3 (Layer Reflectivity Maximum above 33,000 ft MSL, National Weather Service 2009a), indicating high values well above the -20°C level (~24,000 ft MSL). Based on warning experiences in the WGB, this and the numerous pixels of high resolution VIL (National

Weather Service 2009b) above 80 units are both reliable indicators of a severe storm with large hail potential. Using the same ratio of MEHS to actual hail size at the Highway 50 storm survey site, the MEHS of 4.49 inches (11.4 cm) at 21/2301 would correlate to 2.5" diameter (6.4 cm, tennis ball size) observed hail at this time. Granted there would be a high amount of uncertainty in this estimate. It would have been fascinating to hike into the remote Stillwater Range to see if markings of very large hail impacting the ground were visible, however no attempt was made.

b. The "Left Mover"

This storm (#5 in Fig. 1) initially developed between 21/2113 and 21/2121 on the east side of the Pine Nut Mountains. Shortly thereafter a cell split occurred (Fig. 18a); with the left moving updraft continuing up the east edge of the Pine Nuts associated with easterly upslope flow. The storm demonstrated an astonishing collapse as the cell moved northward into the Carson River Valley around 21/2222 (Fig. 18b). This is likely due to a sudden drop-off in orographic lift. Once the remnant cells began interacting with the larger Virginia Range, the storm redeveloped rapidly. This intensification was likely a combination of orographic forcing and enhanced convergence associated with the leading edge of diurnal westerly winds (gusting to ~20 mph, 8.9 m s^{-1}). These winds, referred to as the Washoe Zephyr (Kingsmill 2000), are a regular occurrence in the summer generated by strong thermal contrasts between the Sierra Nevada and the western Nevada deserts. A fast loop of low-level degree reflectivity (Fig. 19) shows numerous small and faint plumes of dust swirling northwest of Reno, NV (strands of low reflectivity). These plumes quickly develop an eastward expansion associated with the increased westerly winds after 21/2200. Fast-looping radar and satellite data can often make boundaries and cell morphology more detectable compared to normal-speed looping or stepping.

The storm continued past the Reno (KRGX) radar site on Virginia Peak and then turned more northwestward at 21/2331 along the Pah Rah Range. Based on the fact the storm followed three separate mountain ranges, and lost cohesion quickly when orographic forcing was lost earlier over the Carson River valley, it is asserted this cell was not necessary a left-moving supercell but was rather strongly tied to the terrain. There is also no evidence of a circulation (cyclonic or anticyclonic) aloft; therefore this storm can be described as a persistent multi-cell. It is also relevant to note the more right-moving supercell storms were able to sustain themselves across large valleys, compared to this storm which lost its original structural characteristics when crossing a single valley.

c. Fallon Mesocyclone

Several credible funnel cloud reports were received in association with one of the final severe storms of the day, which moved directly over Fallon, NV (#2 in Figs. 1 and 2). In this case two cells merged on the north side of Fallon and weakened rapidly, compared to other storms that day which strengthened due to merger processes.

The most notable aspect of this storm was the pronounced mesocyclone observed by spotters along with associated funnel cloud reports (Fig. 20). At 21/0118, the 1.8 degree velocity slice shows a weak cyclonic circulation at 12,000 feet AGL (3.7 km), which is consistent with observations of a mesocyclone at the base of the storm (Fig. 21). High cloud bases likely contributed to the fact these funnels did not touch down. As is typical with high DCAPE desert environments, this storm produced isolated damaging wind southwest of Fallon (several trees blown down but no structural damage). However, there was no discernable velocity signature on the lowest slice indicative of intense straight-line winds or a rear-flank downdraft.

4. Concluding Comments

It is days like this that make forecasters realize the importance of focusing on high impact events and improving upon model forecasts when it counts the most. While there are a plethora of tools, both observed and modeled, an *in-situ* sounding remains one of the single most valuable pieces of data for forecasters. Asynoptic ACARS aircraft soundings (Lese and Ammerman 2008) are available from flights arriving and departing the Reno-Tahoe International Airport, though these nearly always lack critical moisture data. The 1800 UTC sounding as shown in this case: 1) gave forecasters a clear sample of the pre-convective environment shortly before CI, and 2) showed trends in shear, instability, moisture profiles compared to earlier soundings. In the Reno FA, the 1800 to 2100 UTC timeframe is the last chance to capture the pre-CI environment before diurnal downslope westerly winds contaminate the lowest 1-2 km AGL of the sounding.

The usual challenges with respect to severe storm verification in sparsely populated areas continued this day, with storms occurring over very remote areas, with the exception of the Fallon storm. Few spotter reports were received during the event which complicated the warning process. While forecasters at NWS Reno are trained in analyzing supercell radar signatures, such phenomena are rare in the WGB. On this day the warning forecasters tended to err on the side of caution when issuing tornado warnings. Given the uncertainties in mesocyclone detection introduced by the TBSS signal, the mountain-top location of the KRGX radar that yielded limited sampling of the low-levels, and the fact these types of storms are so rare in the WGB, the "subjective threshold" for issuing a tornado warning may have been lower than in the central and eastern CONUS. Being 100% confident the observed circulations were either real or TBSS-induced was not possible during real-time warning operations. It is recommended forecasters always analyze placement of any velocity signature relative to reflectivity features

and spotter reports, and ask, “Does this observation make sense given the conceptual models I know?”

Acknowledgements. I would like to thank the staff at NWS Reno for their dedication during this event and for their enthusiasm in learning about severe convection. Constructive preliminary reviews of this write-up were conducted by Nick Nauslar at Desert Research Institute and Rhett Milne at NWS Reno. I appreciate the thorough formal reviews performed by Randy Graham, NWS Salt Lake City, Steve Corfidi, NWS Storm Prediction Center, and Dr. Pablo Santos, NWS Miami. Their suggestions greatly improved this manuscript.

REFERENCES

Brong, B., 2005: A Study of Flash Flood Potential in Western Nevada and Eastern California to enhance Flash Flood Forecasting and Awareness. M.S. Thesis, University of Nevada-Reno.

CoCoRaHS, 2009: CoCoRaHS Hail Observations. Last accessed: 31 August 2009. [Available online at http://www.cocorahs.org/Content.aspx?page=hailcoco]

Coniglio, M.C., and S.F. Corfidi, 2006: Forecasting the speed and longevity of severe mesoscale convective systems. Preprints, Severe Local Storms Symposium, Amer. Meteor. Soc., Atlanta, GA, CD-ROM.

Corfidi, S. F., J. H. Merritt and J. M. Fritsch, 1996: Predicting the movement of mesoscale convective complexes. *Wea. Forecasting*, **11,** 41-46.

Gibson Ridge Software, 2009: GRLevel2 Analyst Edition. Last accessed: 27 August 2009. [Available online at http://www.grlevelx.com/]

Grumm, R.H., and R. Hart, 2001: Standardized Anomalies Applied to Significant Cold Season Weather Events: Preliminary Findings. *Wea. Forecasting*, **16**, 736–754.

Kingsmill, D., 2000: Diurnally Driven Summertime Winds in the Lee of the Sierra: the Washoe Zephyr. Preprints, Ninth Conference on Mountain Meteorology, Amer. Meteor. Soc., Aspen, CA, CD-ROM.

Lese, A., and J. Ammerman, 2008: The importance of ACARS data in evaluating the near-storm environment of a nocturnal QLCS event. Preprints, 24th Conference on IIPS, Amer. Meteor. Soc., New Orleans, LA, [Available online at http://ams.confex.com/ams/88Annual/techprogram/program_436.htm]

Lozowski, E.P., and G.S. Strong, 1978: On the Calibration of Hailpads. *J. Appl. Meteor.*, **17**, 521–528.

Markowski, P.M., J.M. Straka, and E.N. Rasmussen, 2002: Direct Surface Thermodynamic Observations within the Rear-Flank Downdrafts of Nontornadic and Tornadic Supercells. *Mon. Wea. Rev.*, **130**, 1692–1721.

Milne, R., 2004: A Modified Total Totals Index for Thunderstorm Potential Over the Intermountain West. *Western Region Technical Attachment No. 04-04*, June 15, 2004.

National Weather Service, 2009a: Distance Learning Operations Course, Topic 5, Lesson 12: Layer Composite Reflectivity Maximum. Warning Decision Training Branch. Last accessed: 27 August 2009. [Available online at http://wdtb.noaa.gov/courses/dloc/index.html]

National Weather Service, 2009b: Distance Learning Operations Course, DLOC Topic 5, Lesson 9: Digital Vertically Integrated Liquid. Warning Decision Training Branch. Last accessed: 27 August 2009. [Available online at http://wdtb.noaa.gov/courses/dloc/index.html]

Smallcomb, C., 2006: Hail Spike Impacts on Doppler Radial Velocity Data During Several Recent Lower Ohio Valley Convective Events. Preprints, Severe Local Storms Conference, Amer. Meteor. Soc., St. Louis, MO, CD-ROM.

Smallcomb, C., 2008: Hail Spike Impacts on Doppler Radial Velocity Data during Recent Convective Events in the Continental United States. *National Weather Assoc Electronic Journal of Operational Meteorology*, 2008-EJ5, 10 September 2008.

Wallmann, J., 2004: A Procedure for Forecasting Dry Thunderstorms in the Great Basin using the Dynamic Tropopause and Alternate Tools for Assessing Instability. *Western Region Technical Attachment No. 04-08*, August 3, 2004.

TABLES AND FIGURES

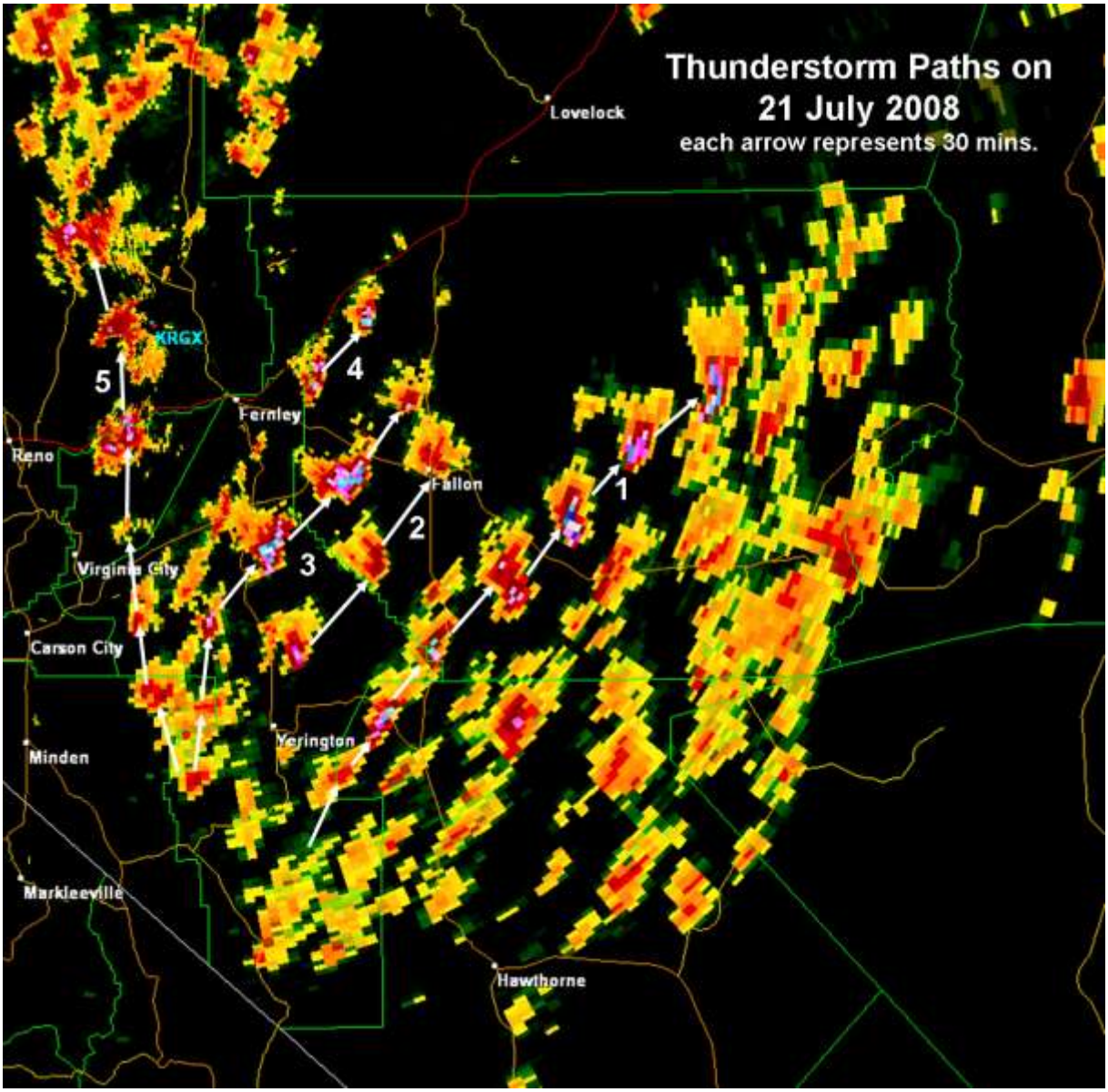

Figure 1. Composite radar map of the five main severe thunderstorm tracks. Numbers refer to individual cells mentioned in the text. The time between each white arrow is 30 minutes. (LINK TO SUMMARY ANIMATION 3.5 MB QuickTime file; for the best view right click and download the file rather than viewing it in the browser)

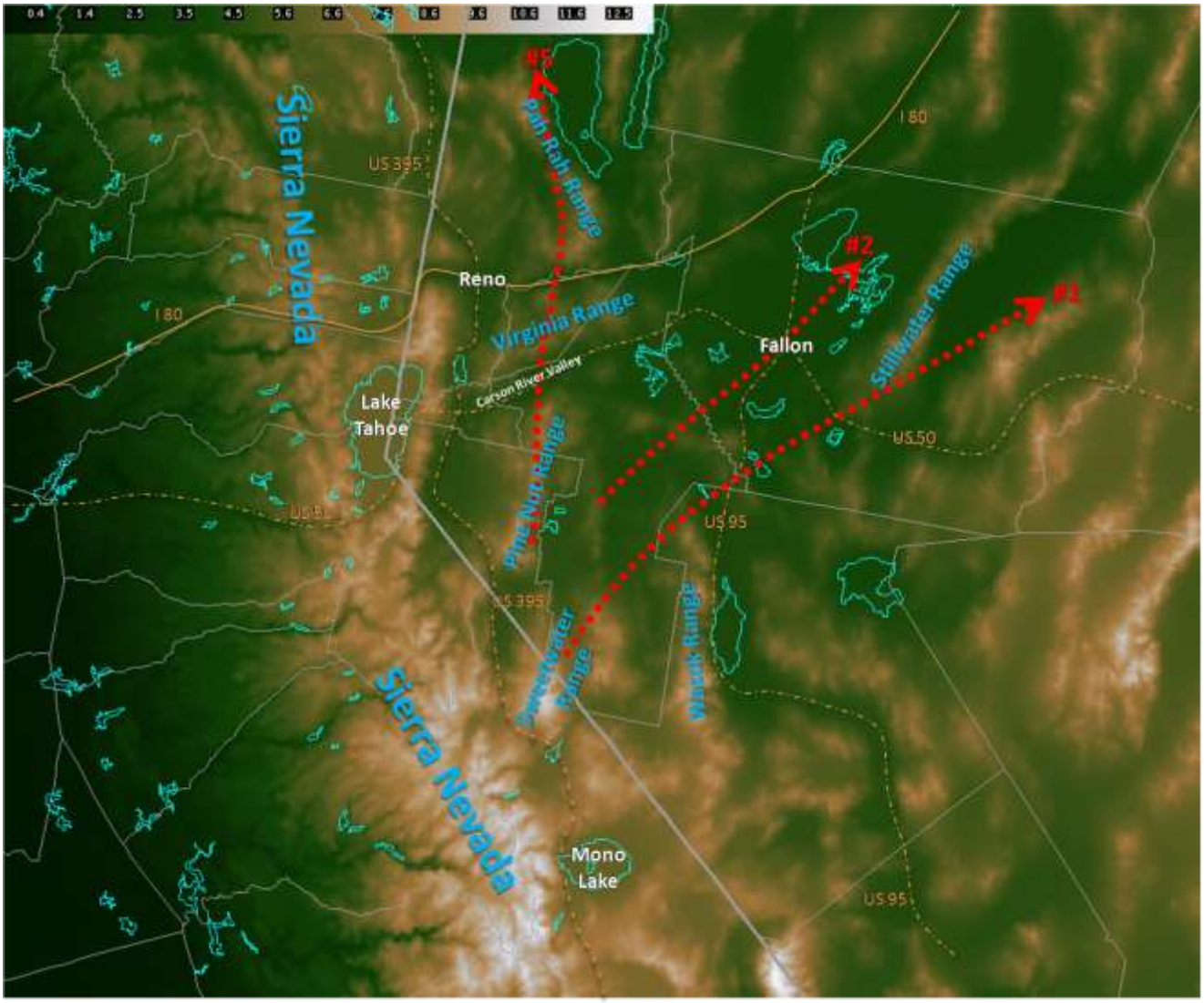

Figure 2. Topographical map of the Sierra Nevada Mountains and far western Nevada. Shading indicates elevation above mean sea level, with legend in upper left (in kft). Individual storms mentioned in the text are highlighted by the red arrows, with numbers corresponding to those in Figure 1. Key locations referenced in the text are noted: mountain ranges in blue; cities, lakes, and valleys in white; and highways as orange lines. Counties are shown in thin gray lines, states in thick gray lines, and lakes in light blue outlines.

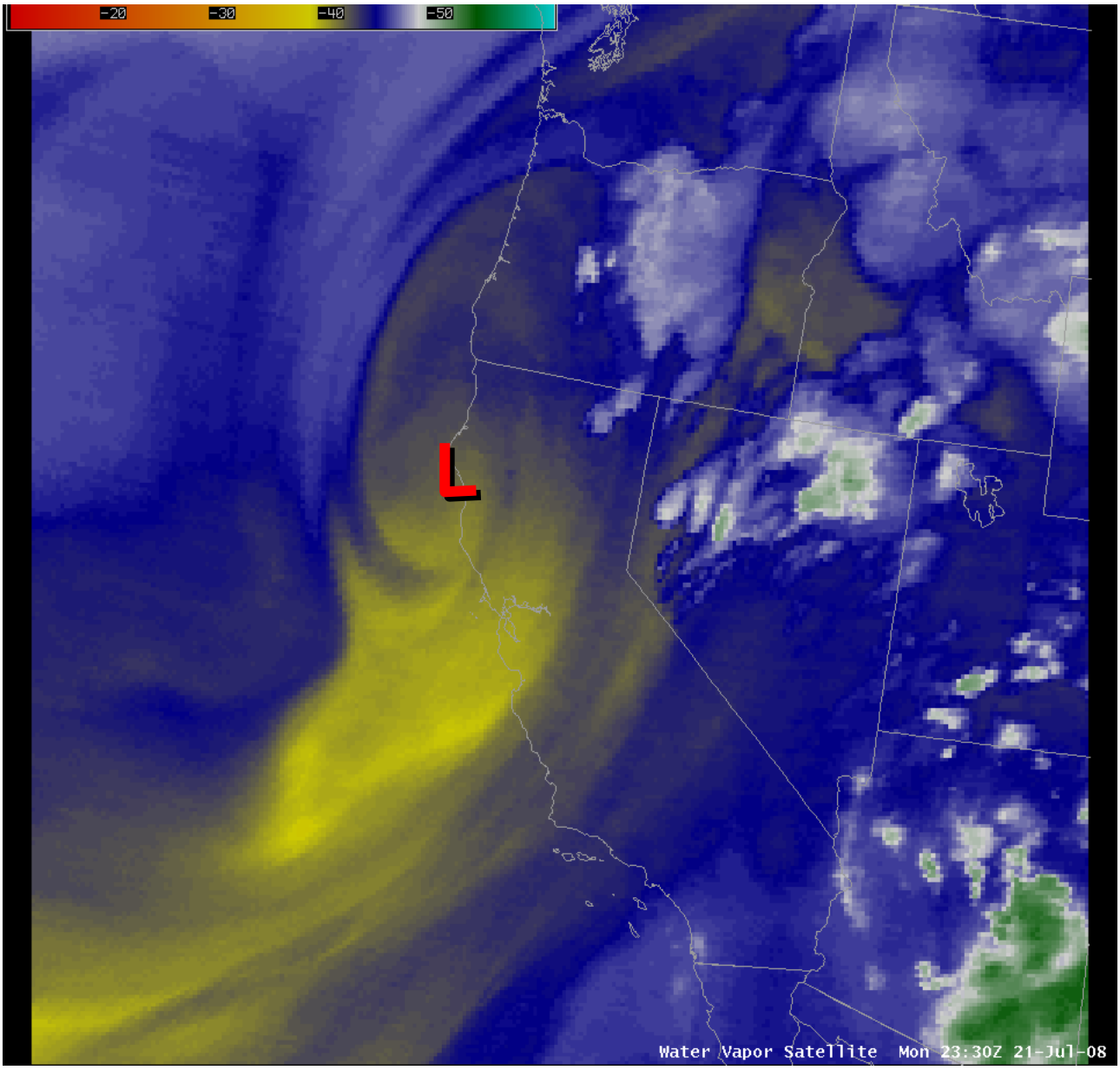

Figure 3. GOES water vapor image valid at 21/2330. Red "L" marks approximate location of the mid-tropospheric circulation center. (LINK TO ANIMATION 1 MB QuickTime file; for the best view right click and download the file rather than viewing it in the browser)

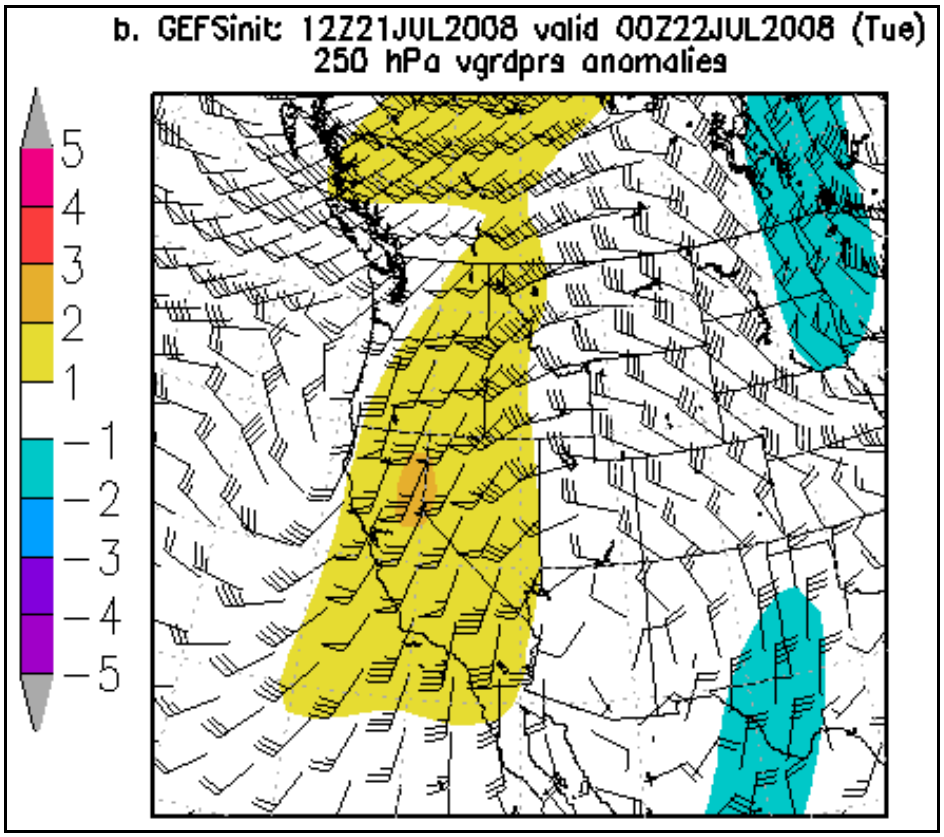

Figure 4. 250 hPa meridional-component wind anomalies (standard deviation from normal in sigma units, shading with scale at left) and mean full-wind (barbs) valid at 22/0000, from the 21/1200 GFS Ensemble Forecast System (GEFS).

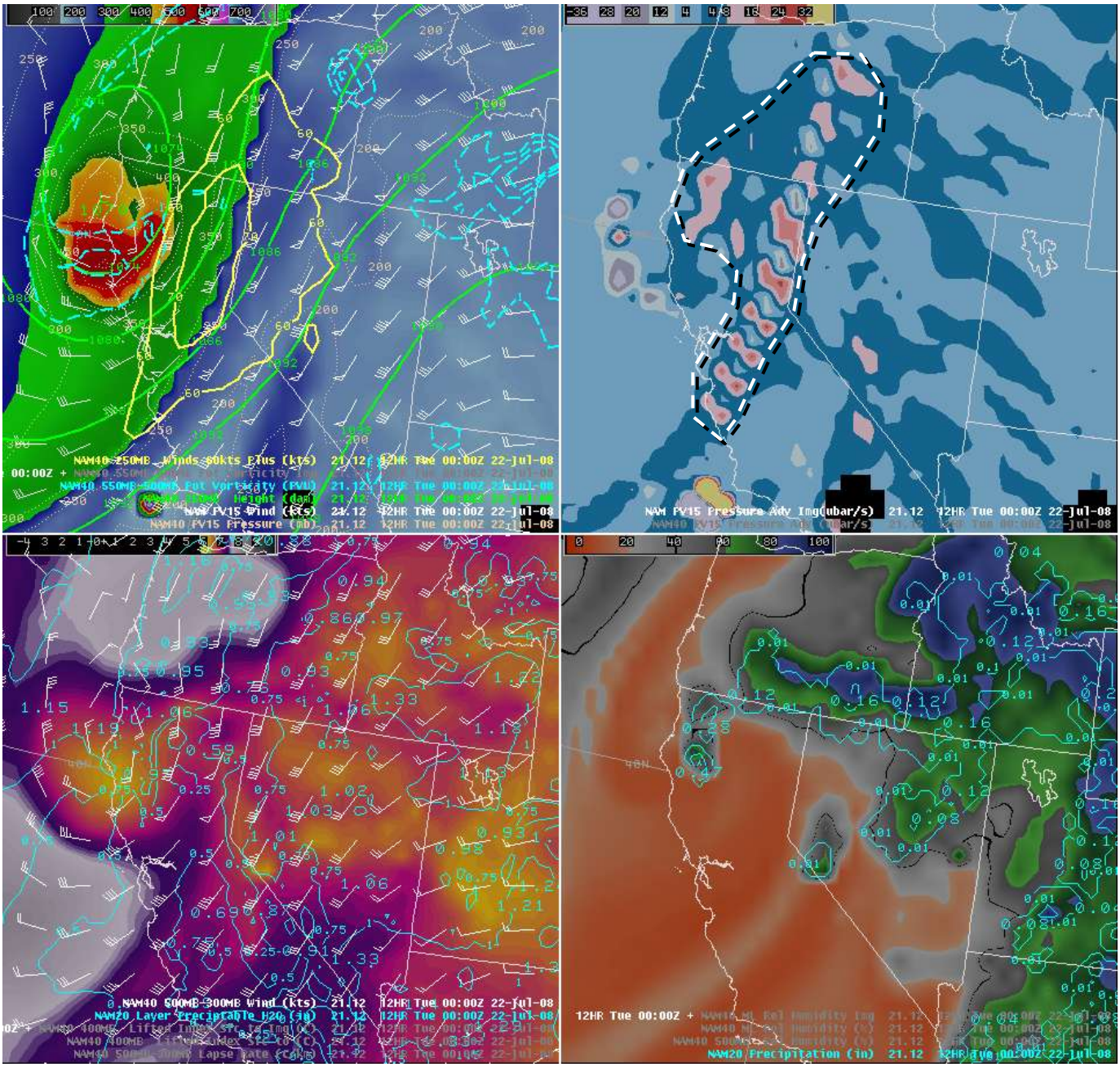

Figure 5. Tropopause procedure valid at 22/0000, from the 21/1200 NAM. Shading legends are in the upper left of each panel. Upper left: 1.5 PVU pressure level shaded (hPa), 250 hPa heights in green (dm), 250 hPa wind speeds above 60 knots (31 m sec^{-1}) in yellow, 550-500 hPa PV above 1 unit in blue, 1.5 PVU surface wind barbs (kts). Upper right: Pressure advection on the 1.5 PVU surface shaded (ubar sec^{-1}); positive areas denote upward vertical motion. Area of ascent described in the text is highlighted with the white dashed contour. Lower left: 500-300 hPa lapse rates (C km^{-1}) shaded, precipitable water (in) in blue, 500-300 hPa layer average wind barbs (kts). Lower right: 500 hPa relative humidity shaded, 3-hour accumulated precipitation in blue.

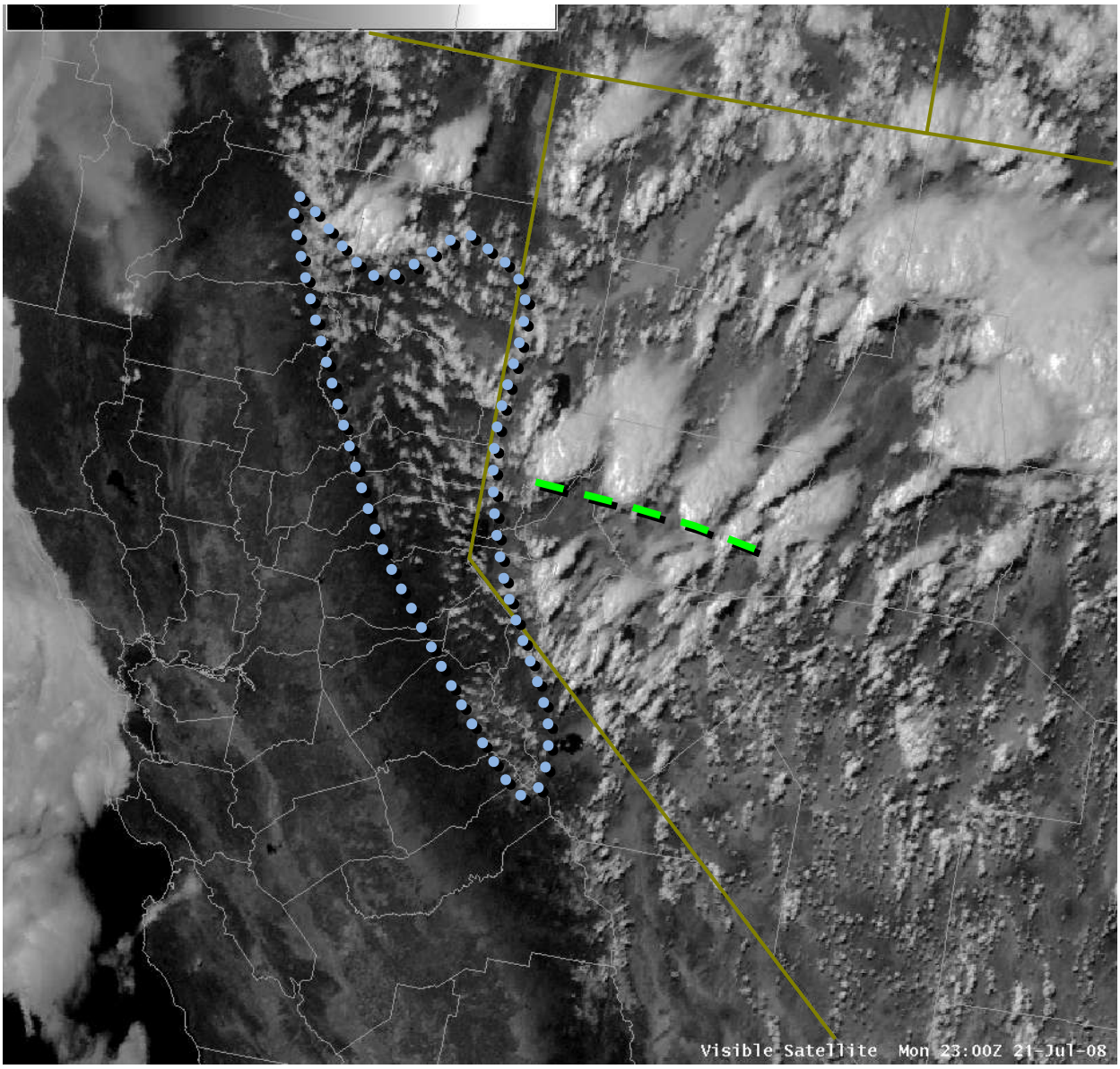

Figure 6. Regional visible satellite valid at 21/2300. Presumed boundary that primary storms developed along is highlighted with the green dashed line. Area of wave clouds (implying the presence of a stable layer) outlined in blue dotted line. County outlines in gray, state border in dark yellow. (LINK TO ANIMATION 16 MB QuickTime file; for the best view right click and download the file rather than viewing it in the browser)

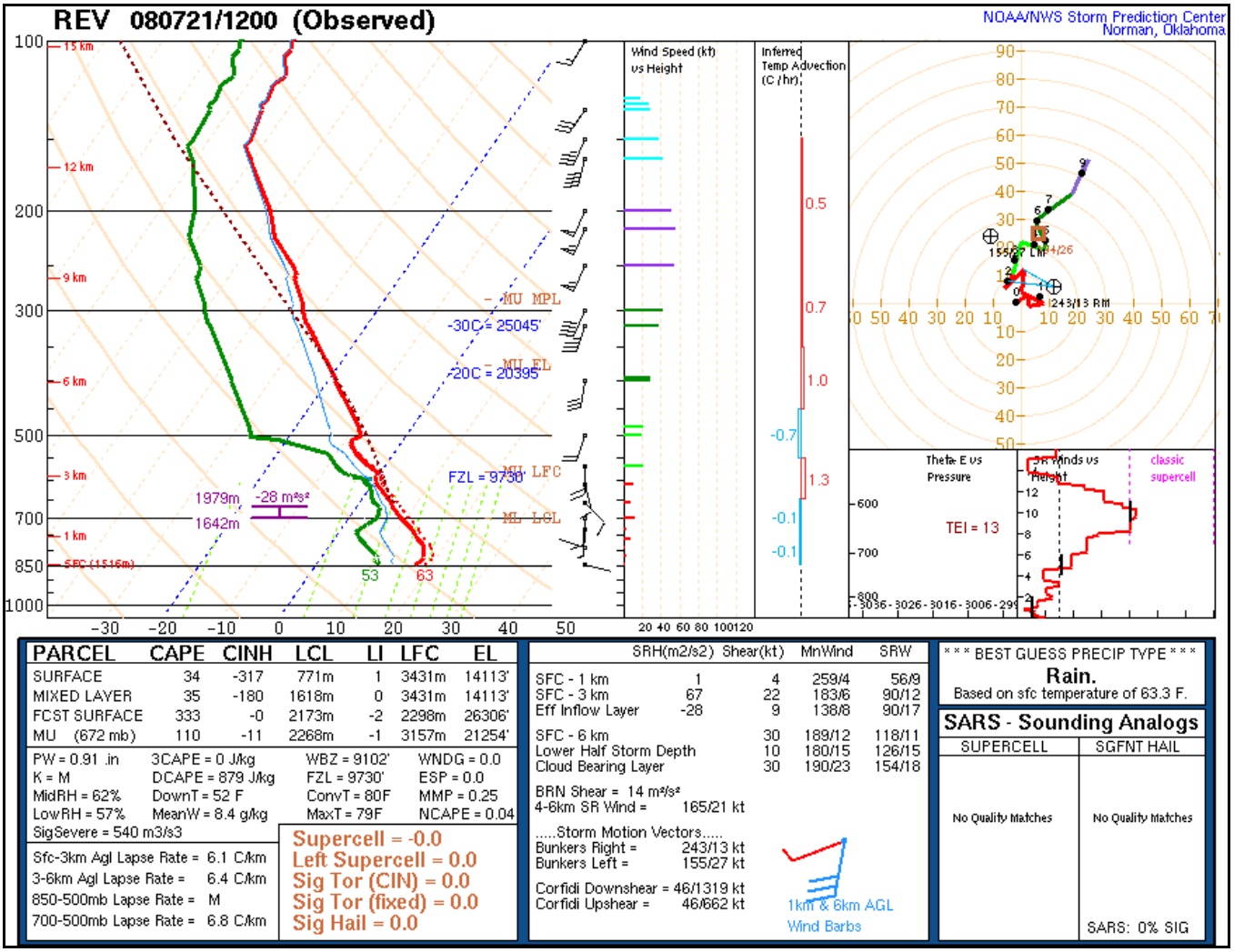

Figure 7. Observed soundings from Reno, NV (KREV) valid at 21/1200 to 22/0000. Source: NOAA/NWS Storm Prediction Center website. (LINK TO COMPLETE SOUNDING SEQUENCE Java animation will open in browser)

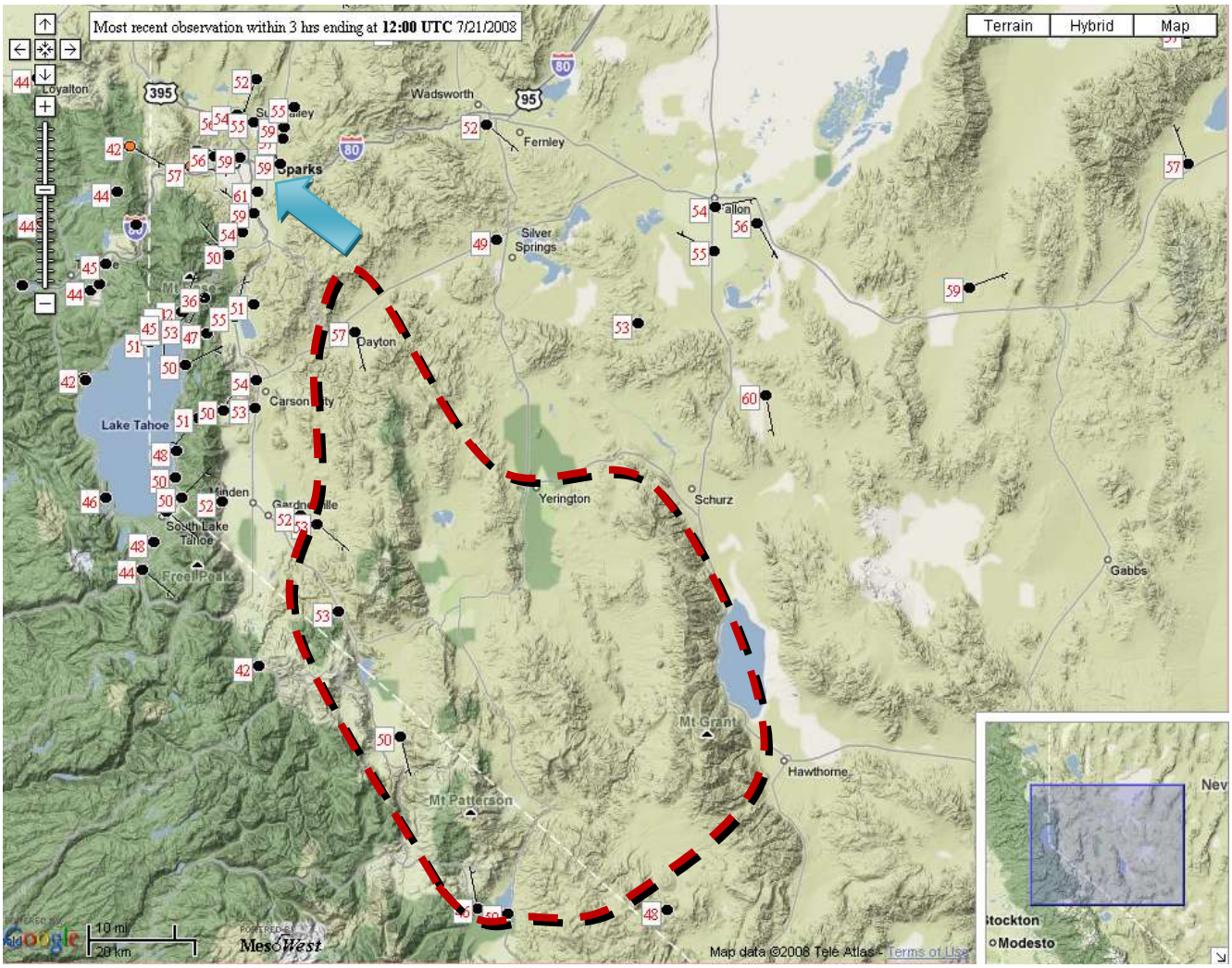

Figure 8. MesoWest surface dewpoint (°F) and wind barb plot (MPH) valid at 21/1200. Map displays the most recent observation within a three-hour window ending at 21/1200, which can help display remote data that has a significant time lag. The Reno-Sparks metropolitan area is located at the tip of the blue arrow. The general area of CI is noted by the dark red dashed line.

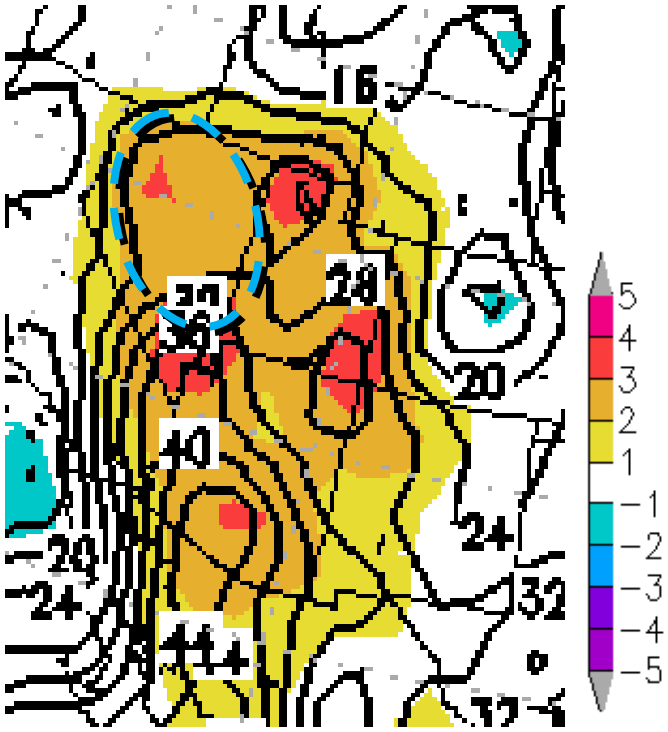

Figure 9. Precipitable water (PW) anomaly field based on the GEFS mean, analysis valid at 21/1200. Shading represents standard deviation from normal in sigma units, with black lines delineating the mean (mm). The blue dashed circle highlights the area being discussed in the text.

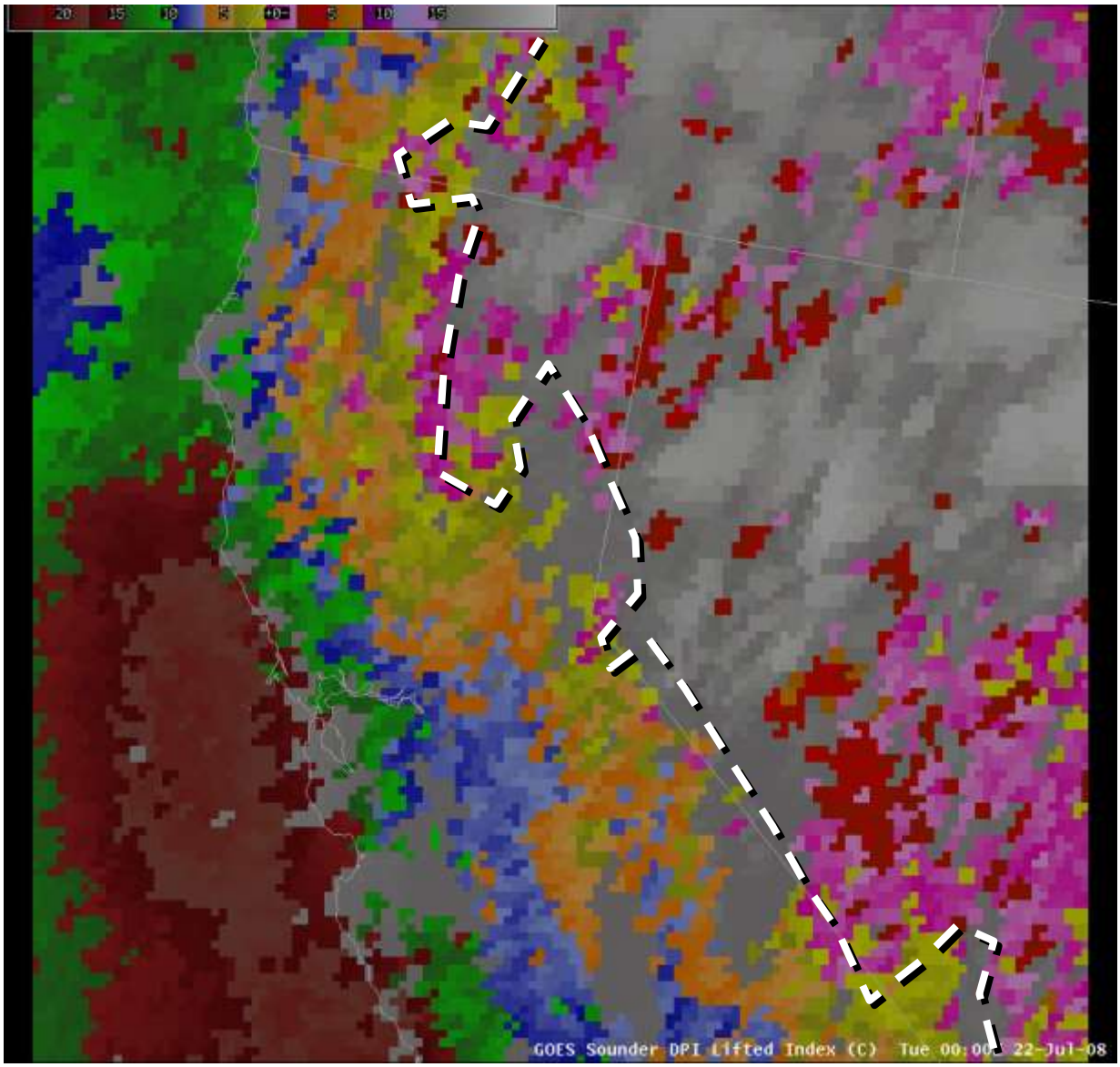

Figure 10. GOES sounder surface based lifted index (shading, °C) valid at 22/0000. White dashed line marks the approximate location of the 0°C contour.

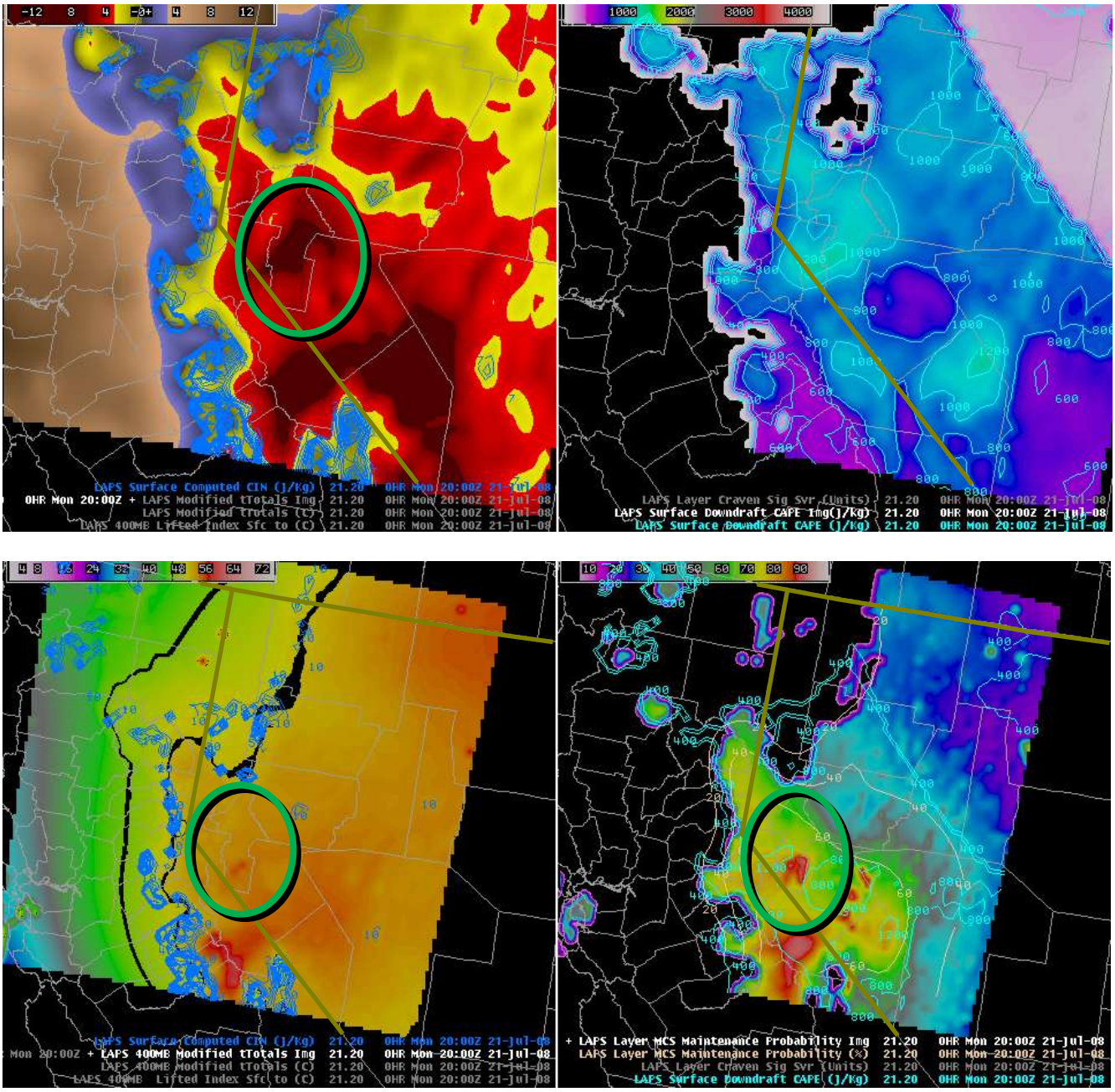

Figure 11. LAPS analysis valid at 21/2000. Shading legends are in the upper left of each panel. Upper Left: Surface based LI to 400 hPa (C) in shading with areas of surface based CIN (J kg^{-1}) in blue. Upper Right: Downdraft CAPE (J kg^{-1}) in shading and blue lines. Lower Left: Modified Total Totals to 400 hPa (C) in shading with critical thresholds for thunderstorm development noted by black stripes (approximately 45 and 51 ºC), surface based CIN (J kg^{-1}) in blue. Lower Right: MCS Maintenance Probability in shading (%), Craven-Brooks Significant Severe parameter in light green (every 5 units starting at 10), and downdraft CAPE (J kg^{-1}) in blue. CI area discussed in text highlighted by the green oval. County outlines in gray, state border in dark yellow.

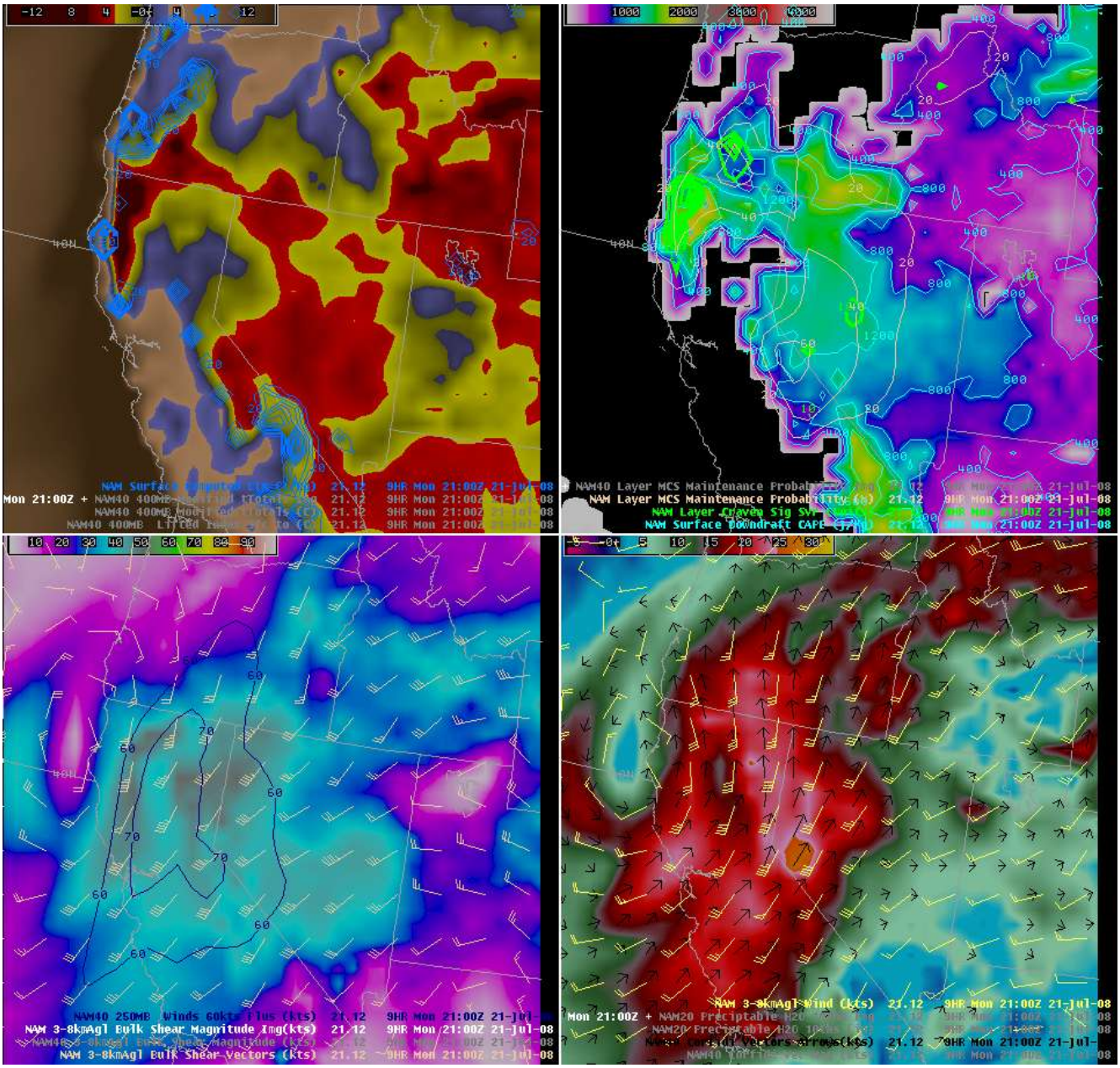

Figure 12a. Severe weather model procedure used at NWS Reno. 21/1200 NAM 9-hour forecast valid at 21/2100. Shading legends are in the upper left of each panel. Upper left: Surface based LI to 400 hPa (C) in shading with areas of surface based CIN (J/kg) in blue. Upper right: Downdraft CAPE (J kg^{-1}) in shading and blue lines, Craven-Brooks Significant Severe parameter in light green (every 5 units starting at 10), and MCS Maintenance Probability (%) in light brown. Lower left: 3-8km AGL bulk shear (kts) in shading, 250 hPa wind speeds (kts, above 60) in dark blue, and 3-8km AGL bulk shear barbs. Lower right: "Modified" Corfidi Vectors (black vectors) and magnitudes (shading, kts), and 3-8km AGL mean wind barbs (kts).

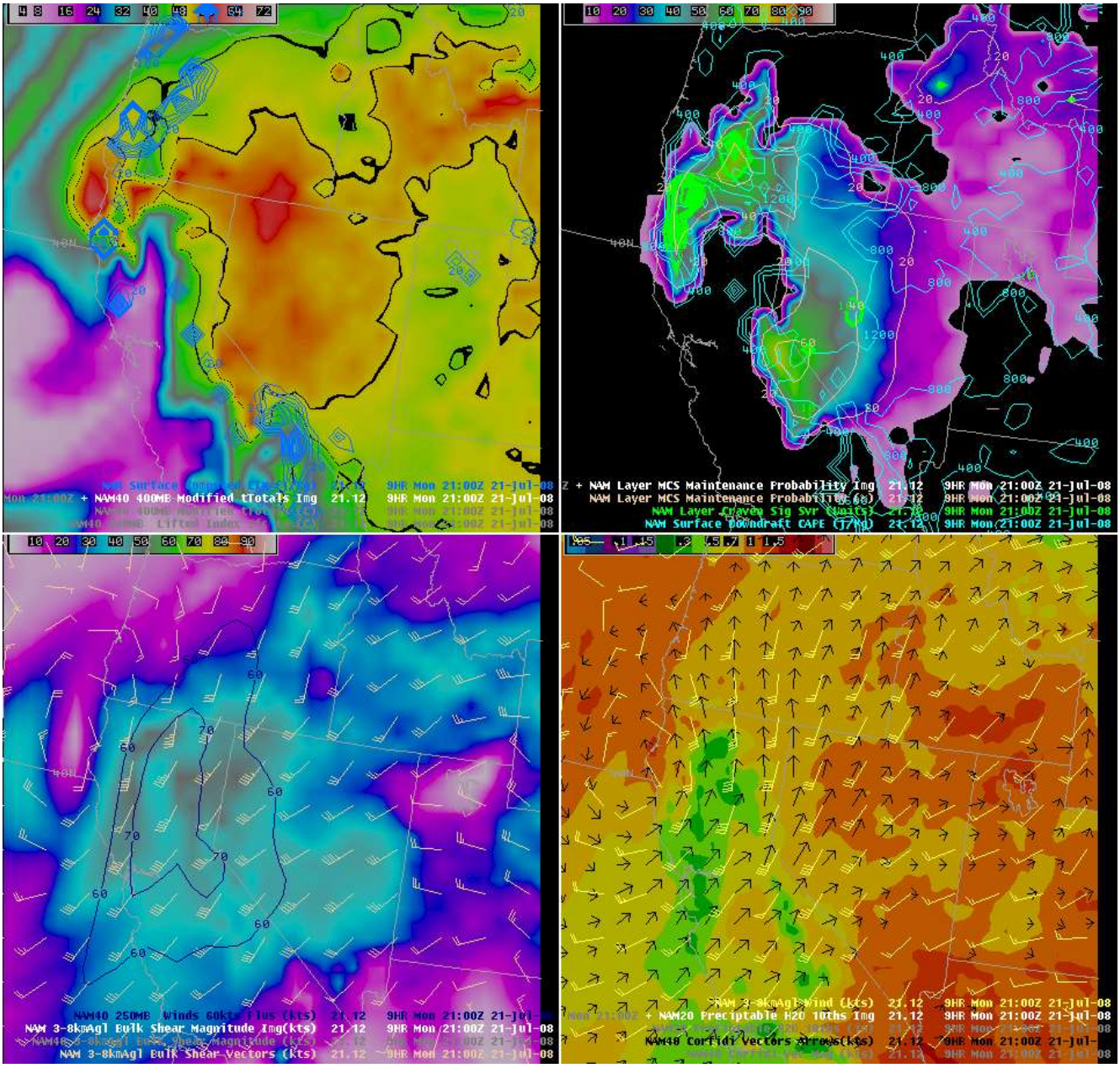

Figure 12b. Continuation of severe weather procedure displayed in Figure 11a, valid at the same time. Shading legends are in the upper left of each panel. Upper left: Modified Total Totals to 400 hPa (C) in shading with critical thresholds for thunderstorm development noted by black stripes (approximately 45 and 51), surface based CIN (J kg^{-1}) in blue. Upper right: MCS Maintenance Probability in shading, Craven-Brooks Significant Severe parameter in light green (every 5 units starting at 10), and downdraft CAPE (J kg^{-1}) in blue. Lower left: 3-8km AGL bulk shear (kts) in shading, 250 hPa wind speeds (kts, above 60) in dark blue, and 3-8km AGL bulk shear barbs. Lower right: Precipitable water (inches) in shading, "modified" Corfidi Vectors in black, and 3-8km AGL mean wind barbs (kts) in yellow.

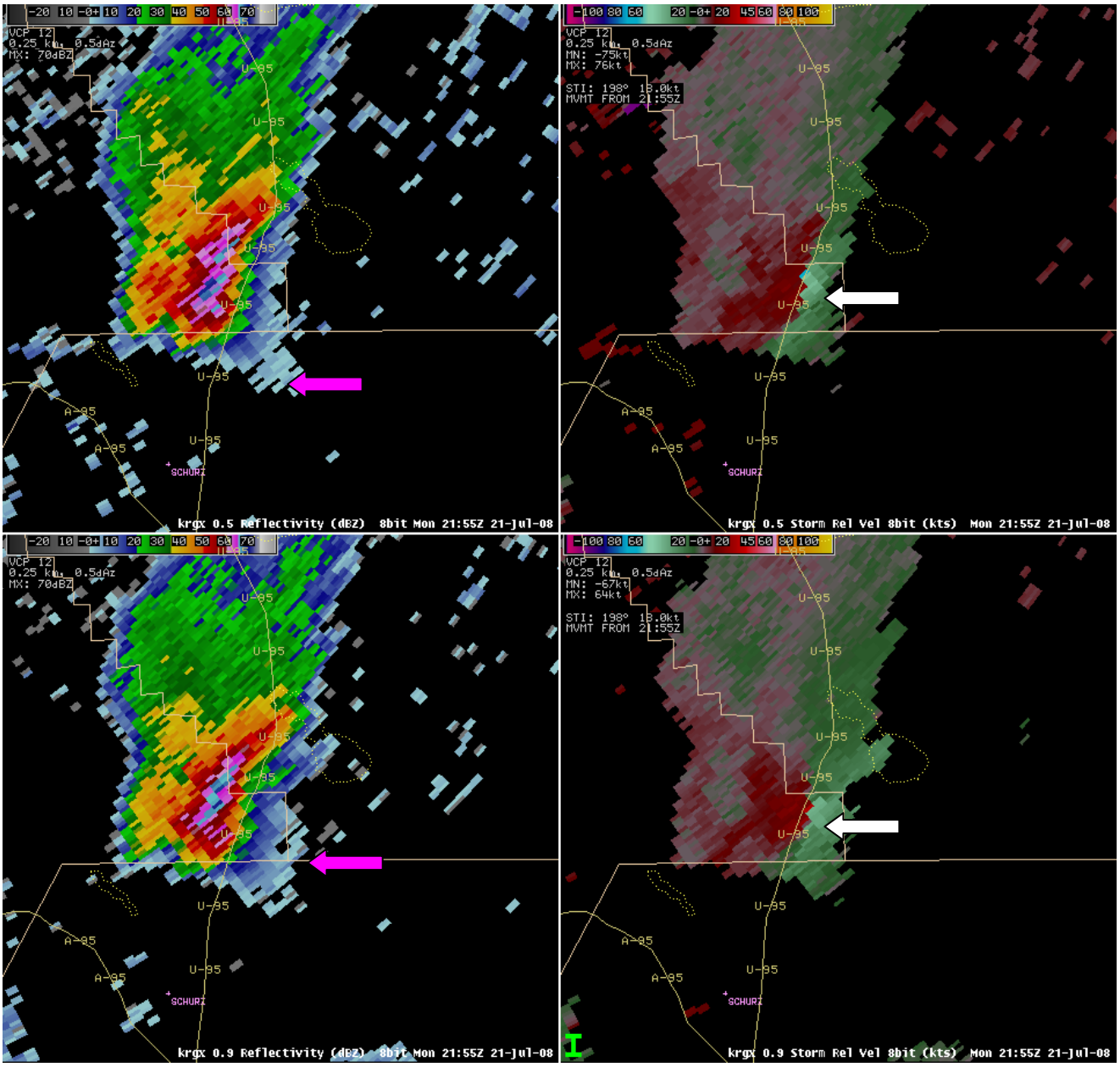

Figure 13a. KRGX WSR 88-D low level reflectivity and velocity data at 21/2155. The storm is cell #1 in Figures 1 and 2. Upper left: 0.5 degree reflectivity. Upper right: 0.5 degree storm relative velocity (kts). Lower left: 0.9 degree reflectivity. Lower right: 0.9 degree storm relative velocity. Areas of interest referred to in text highlighted by pink (TBSS) and white (velocity circulation) arrows. Color scales located in upper left of each panel. County lines in light brown, highways in tan, town names in pink, and lake (often dry) outlines in yellow dotted lines. 0.5 degree beam altitude at white arrow head: 13,200 ft MSL (8,800 ft or 2.7 km AGL).

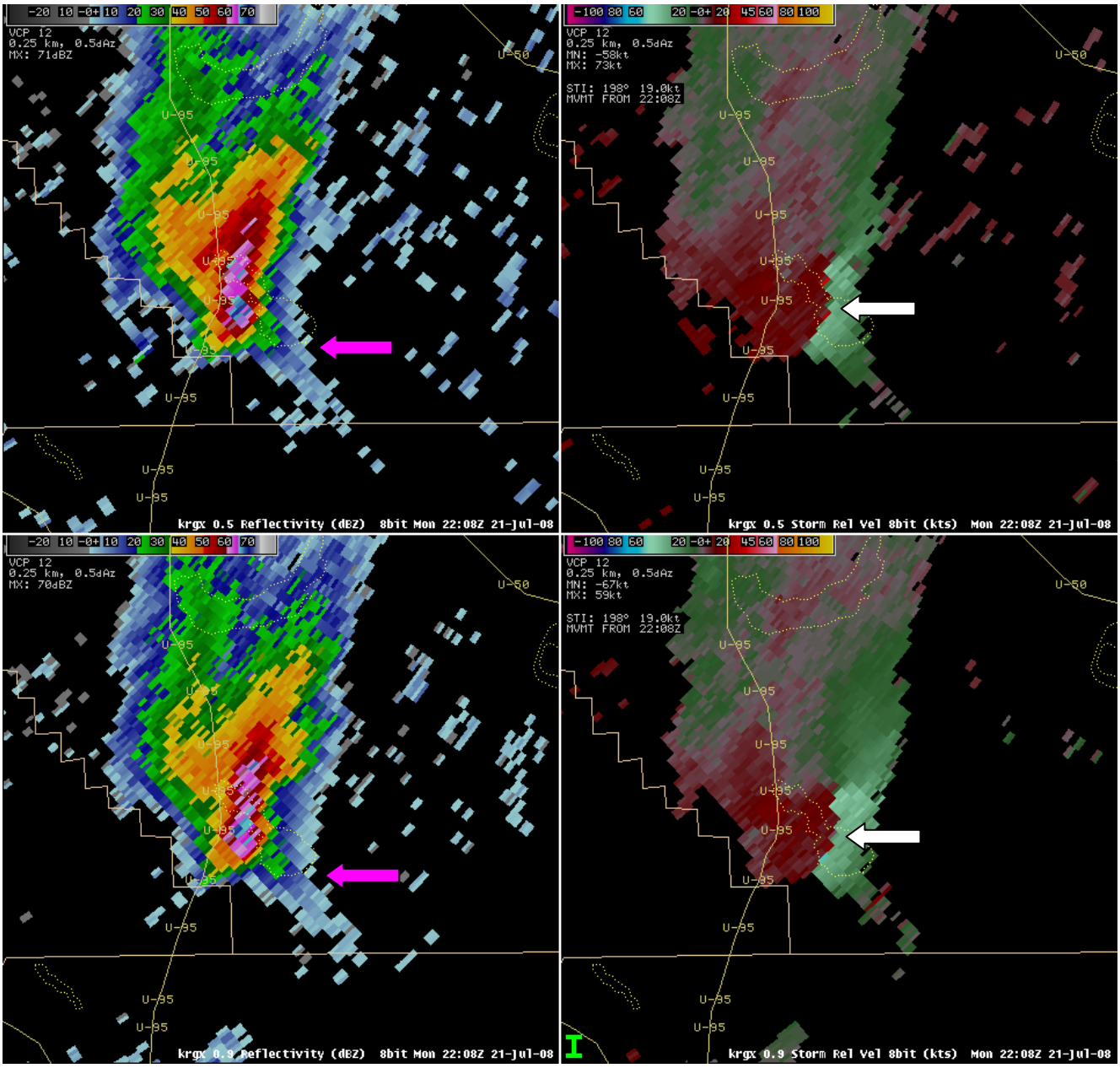

Figure 13b. As in Figure 12a, except at 21/2208. 0.5 degree beam altitude at white arrow head: 12,700 ft MSL (8,700 ft or 2.6 km AGL).

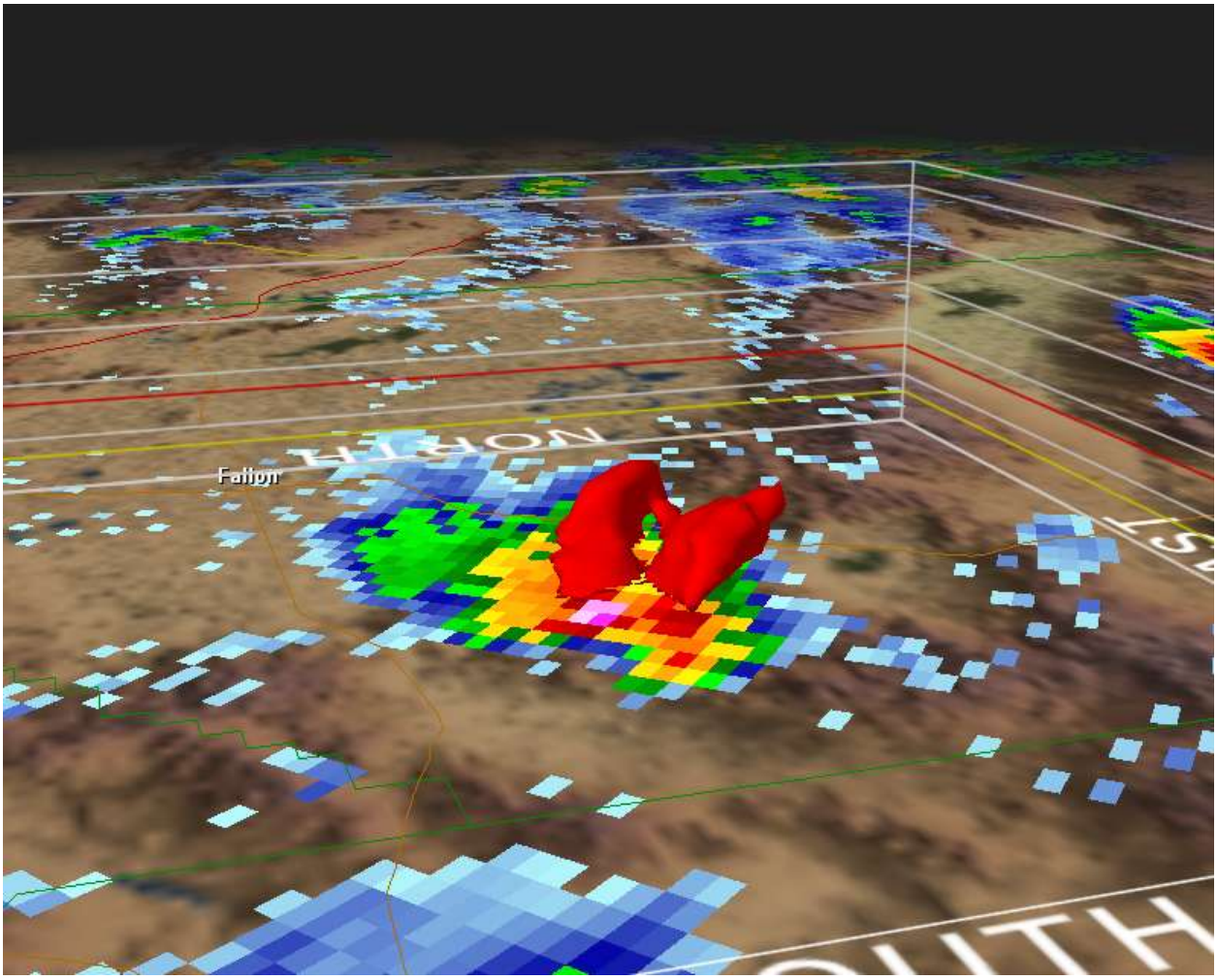

Figure 14. Rendition of the 50 dBz isosurface at 21/2226 from KRGX WSR-88D data. The storm is cell #1 in Figures 1 and 2. (LINK TO ANIMATION 2.5 MB QuickTime file; for the best view right click and download the file rather than viewing it in the browser)

Figure 15. Photos of the hail pock marks (or hail fossils) discovered along US Highway 50 during a storm survey. A quarter (top) and penny (bottom) are shown for comparison.

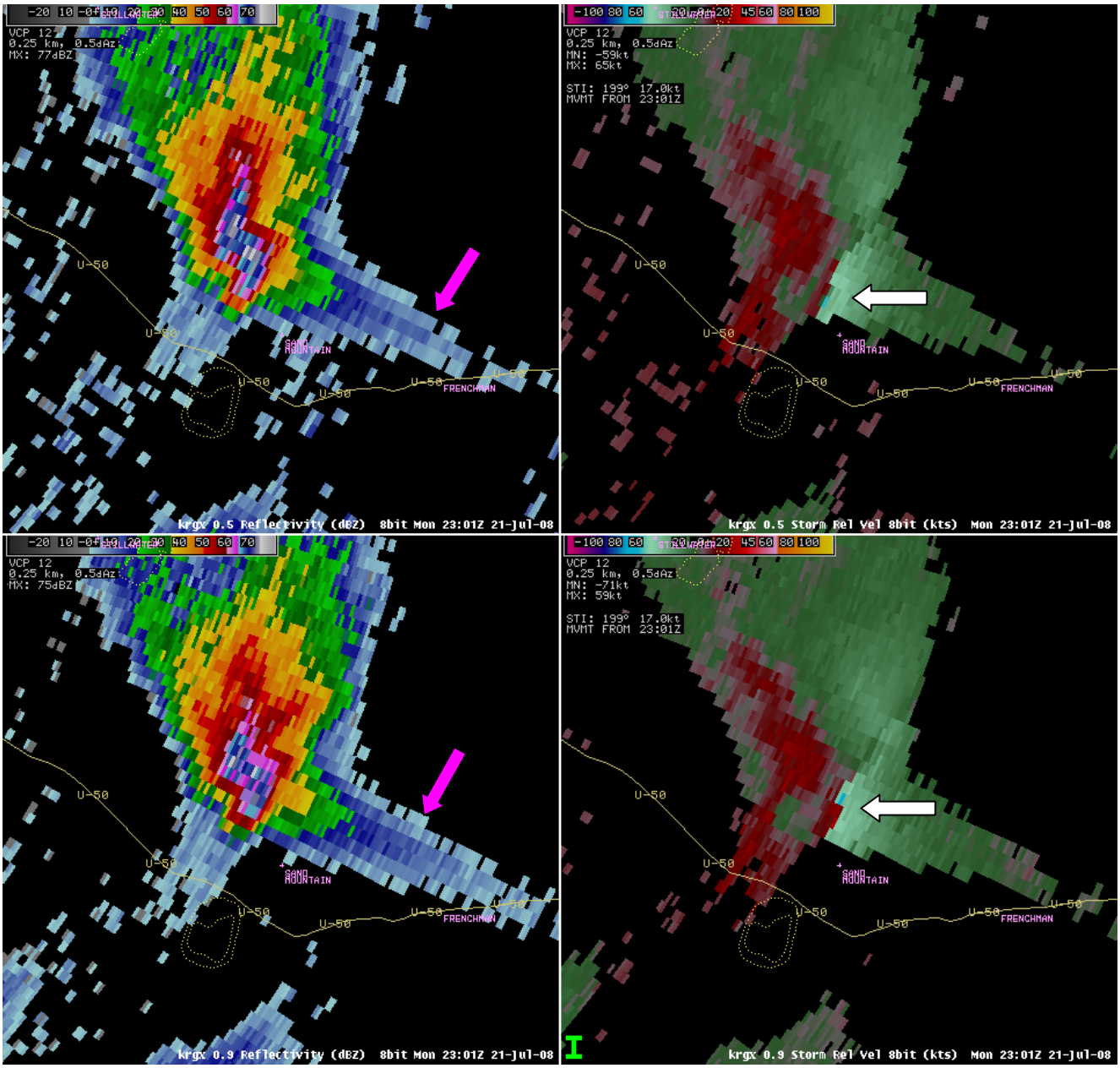

Figure 16. As in Figure 13a, except at 21/2301. 0.5 degree beam altitude at white arrow head: 13,300 ft MSL (8,200 ft or 2.5 km AGL). The storm is cell #1 in Figures 1 and 2.

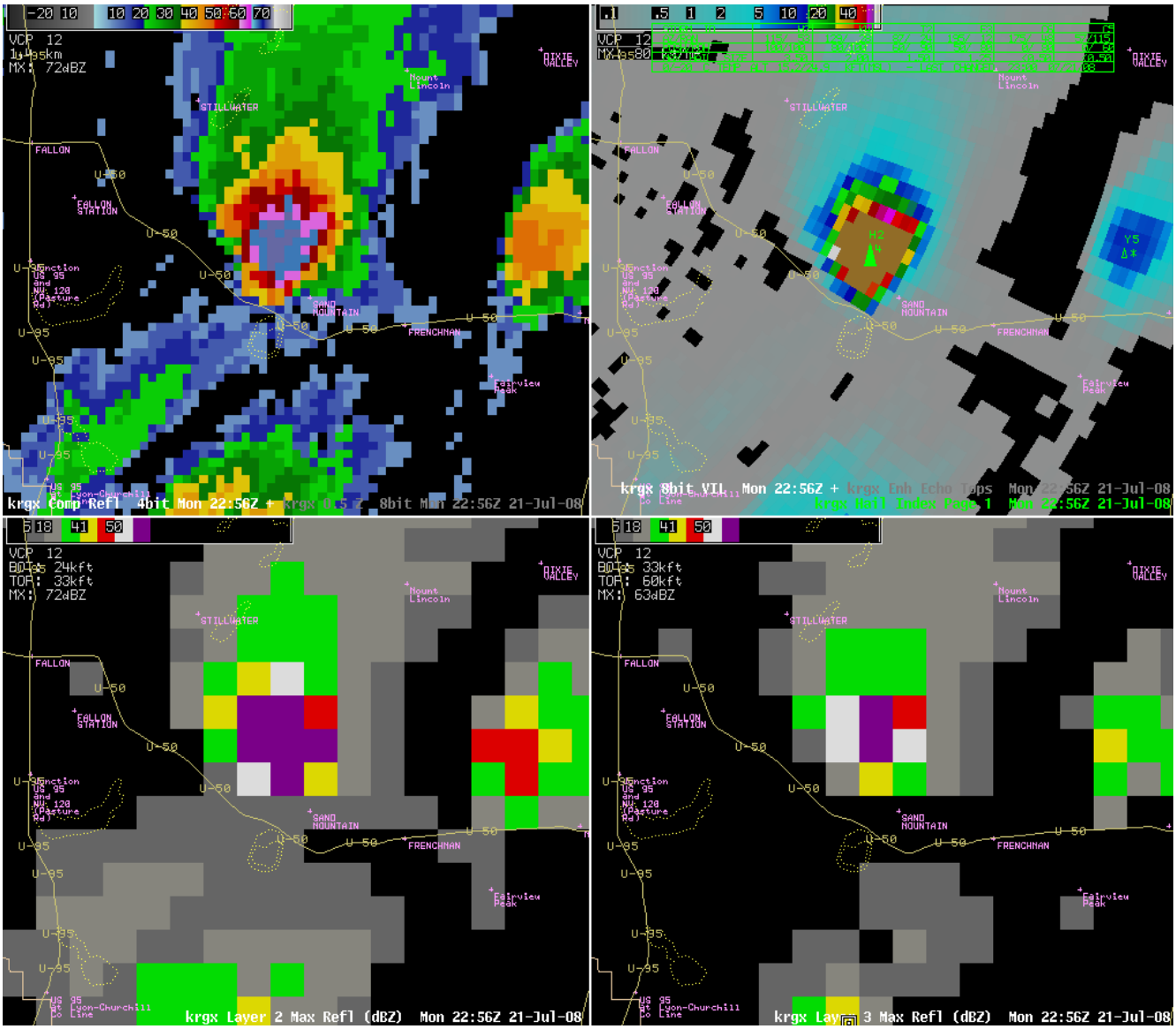

Figure 17. NWS Reno Pulse Severe Storm Procedure valid at 21/2256. The storm is cell #1 in Figures 1 and 2. Upper Left: composite reflectivity. Upper Right: high resolution vertically integrated liquid (VIL) and WSR-88D maximum hail size estimates. Lower Left: layer reflectivity maximum (LRM) between 24-33,000 ft MSL, also known as LRM2. Lower Right: LRM above 33,000 ft MSL, known as LRM3. Highways noted in tan color lines, dry lake beds in yellow dotted lines, and key locations in pink.

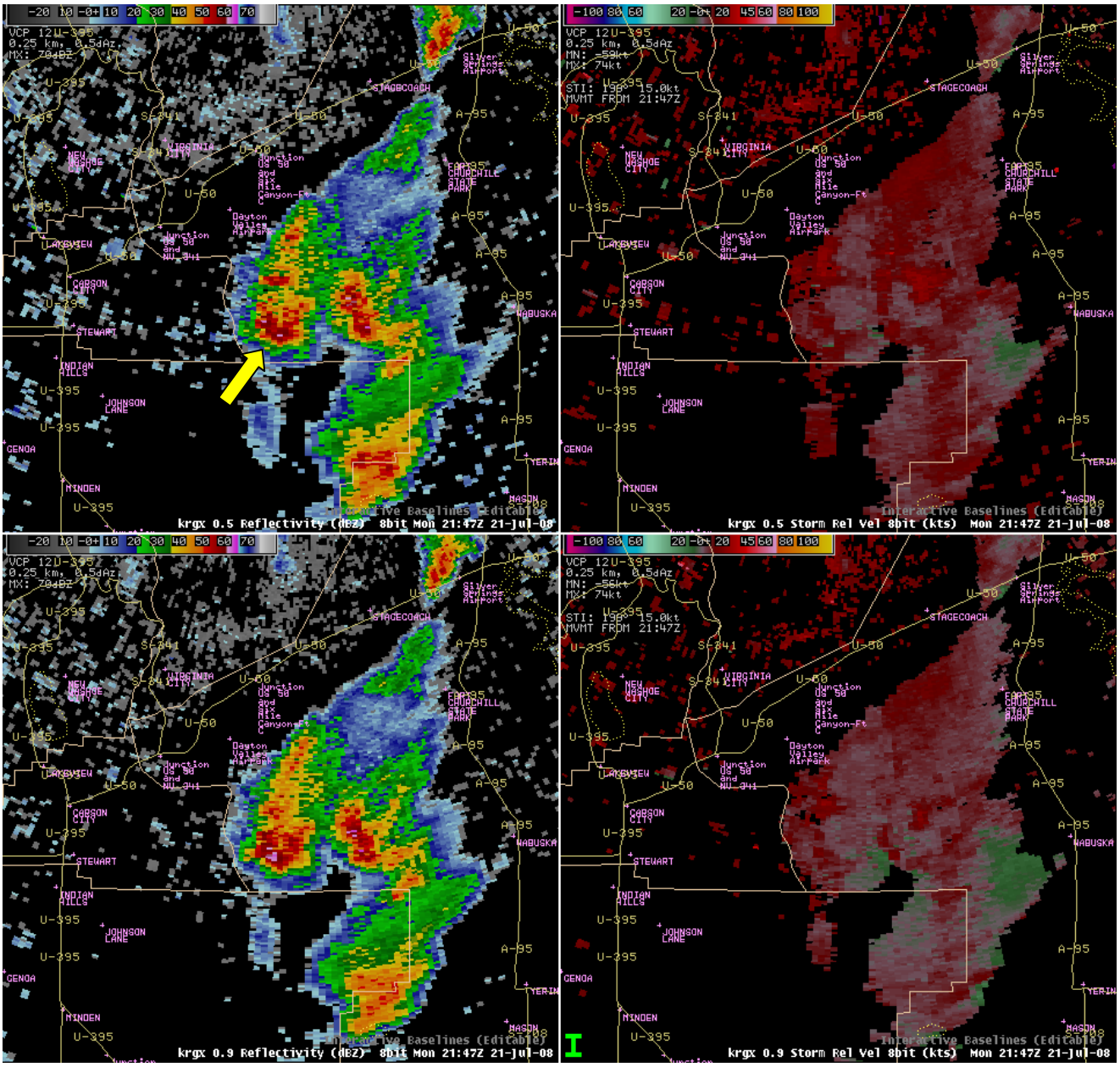

Figure 18a. As in Figure 13a, showing the pre-collapse state at 21/2147, immediately after cell splitting. Yellow arrow denotes the "left mover" storm (cell #5 in Figures 1 and 2). 0.5 degree beam altitude at yellow arrow head: 11,400 ft MSL (4,700 ft or 1.4 km AGL).

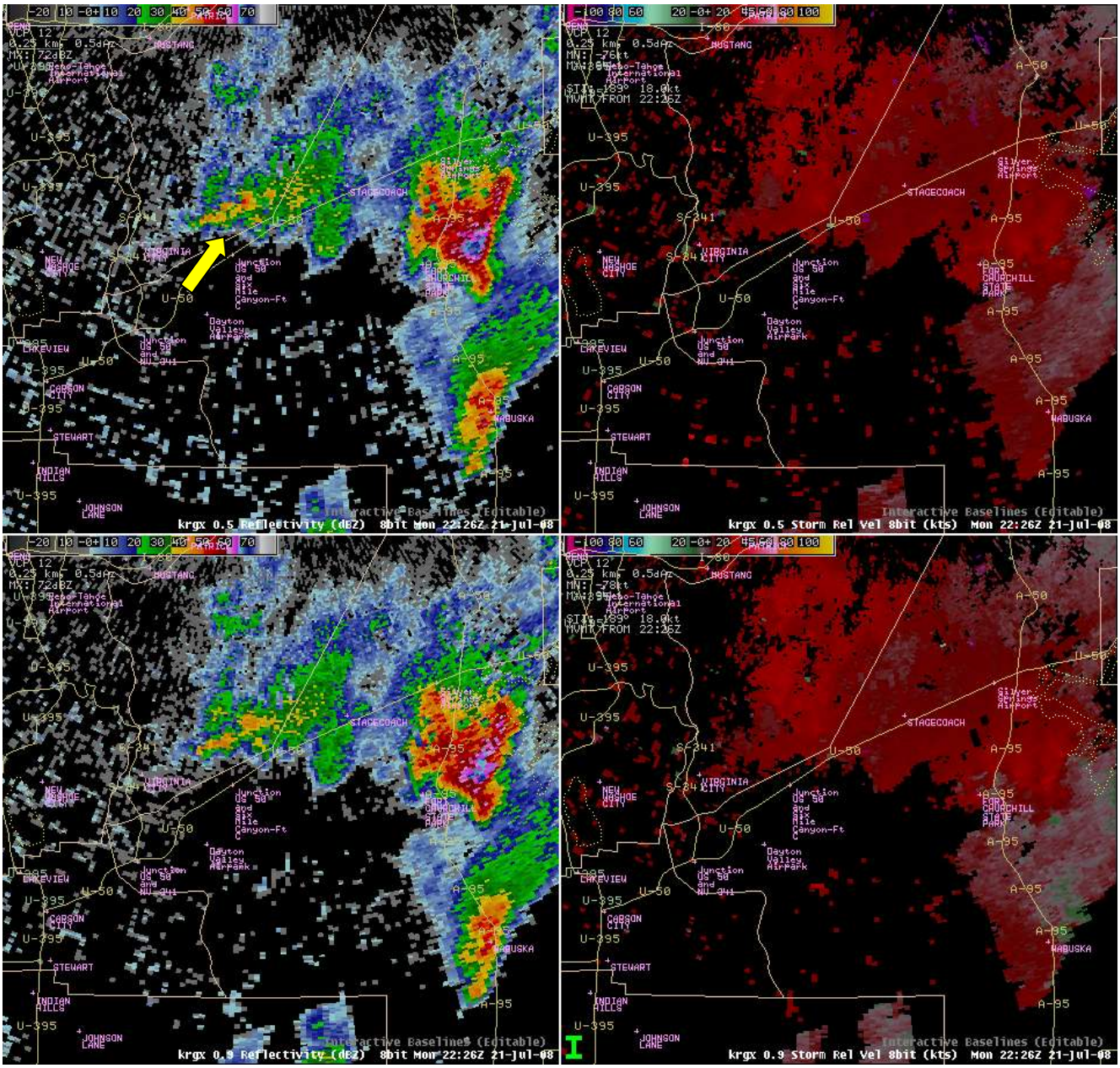

Figure 18b. As in Figure 13a, except at 21/2226. This is the point at which the "left mover" storm was at its weakest. 0.5 degree beam altitude at yellow arrow head: 10,100 ft MSL (5,700 ft or 1.7 km AGL).

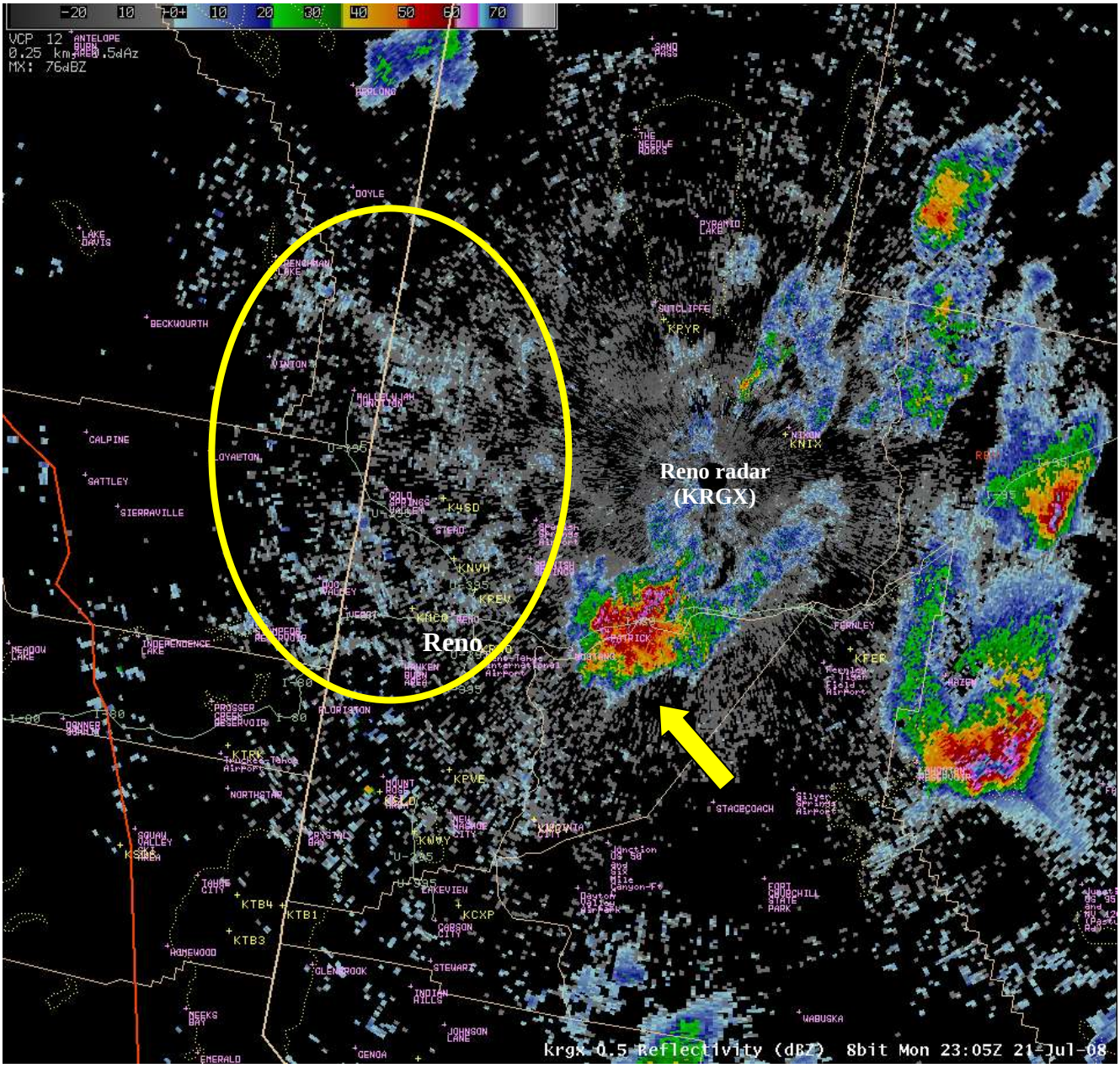

Figure 19. KRGX 0.5 degree reflectivity at 21/2305. Dust plumes noted in the text highlighted with yellow oval. Yellow arrow notes the "left mover" storm (cell #5 in Figures 1 and 2). (LINK TO FAST ANIMATION Large 29 MB QuickTime file; for the best view right click and download the file rather than viewing it in the browser)

Figure 20. NWS Reno Meteorologist, Kyle Mozley, took this picture of a well developed mesocyclone associated with cell #2 (in Figures 1 and 2) passing over Fallon, NV. Kyle noted the base of the cell was rotating cyclonically. Though precipitable water values were well above normal for the region, sufficiently high bases created an LP-supercell look.

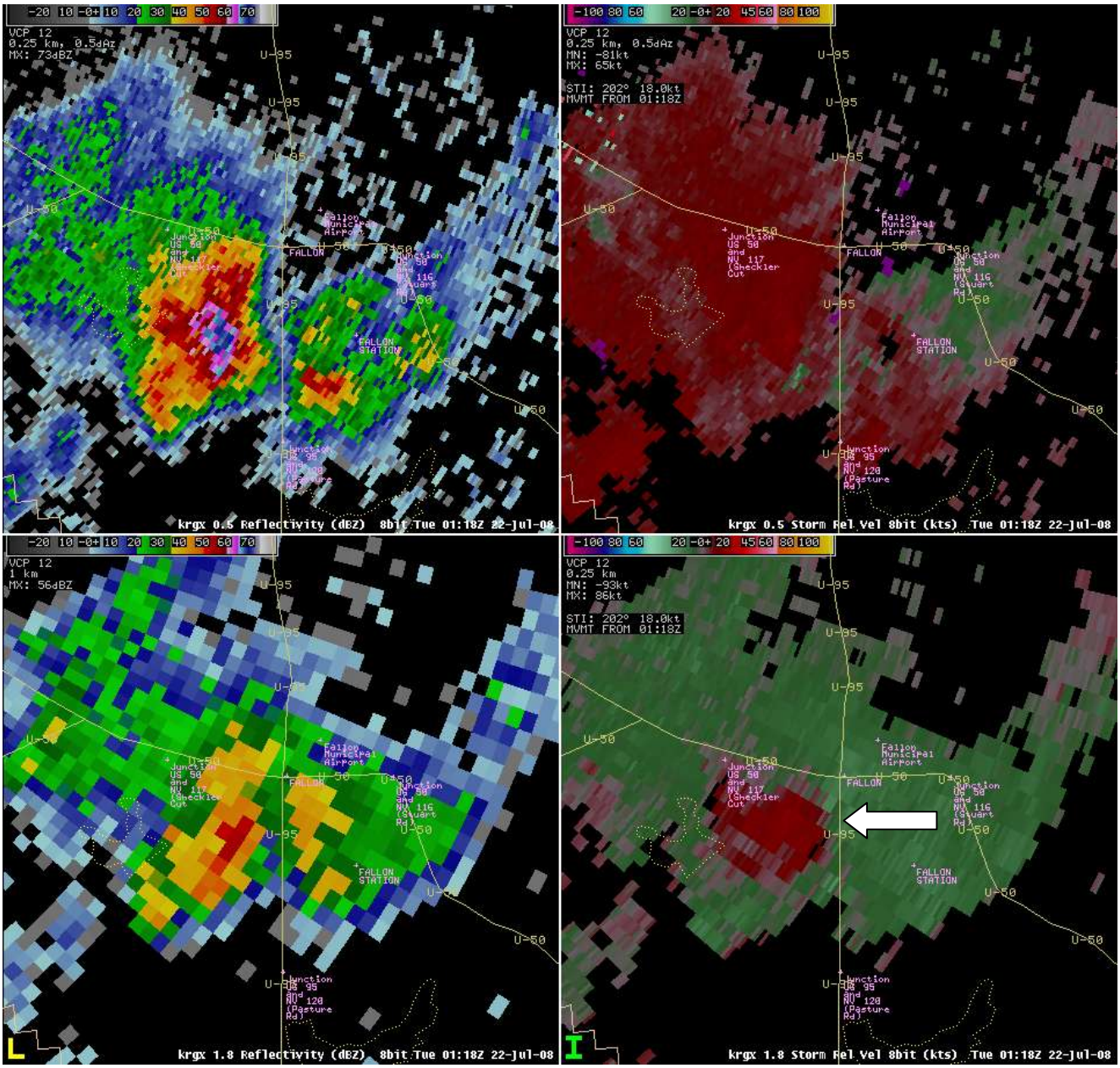

Figure 21. KRGX WSR 88-D low level reflectivity and velocity data at 22/0118. This storm is cell #2 in Figures 1 and 2. Upper left: 0.5 degree reflectivity. Upper right: 0.5 degree storm relative velocity (kts). Lower left: 1.8 degree reflectivity. Lower right: 1.8 degree storm relative velocity. Area of interest referred to in text highlighted by white arrow; elevation of 1.8 degree radar slice at arrow head is 12,000 ft AGL (3.7 km). Color scales located in upper left of each panel. County lines in light brown, highways in tan, town names in pink, and lake (often dry) outlines in yellow dotted lines. The resolution differences between the 0.5 and 1.8 degree reflectivity are attributable to super-resolution being applied to only the lowest three elevation cuts.